

INTERNATIONAL UNION OF PURE AND APPLIED CHEMISTRY
ANALYTICAL CHEMISTRY DIVISION
COMMISSION ON RADIOCHEMISTRY AND NUCLEAR TECHNIQUES*

CRITICAL EVALUATION OF THE CHEMICAL PROPERTIES OF THE TRANSACTINIDE ELEMENTS

(IUPAC Technical Report)

Prepared for publication by
JENS VOLKER KRATZ

Institut für Kernchemie, Universität Mainz, 55099 Mainz, Germany

*Membership of the Commission during the preparation of this report (1998–1999) was as follows:

Chairman: V. P. Kolotov (Russia, 1996–1999); **Secretary:** P. Benes (Czech Republic, 1998–1999); **Titular Members:** H. W. Gäggeler (Switzerland, 1998–1999); J. V. Kratz (FRG, 1998–1999); H. Nakahara (Japan, 1994–1999); **Associate Members:** Z. Chai (China, 1996–1999); Carol H. Collins (Brazil, 1998–1999); A. Vértes (Hungary, 1998–1999); P. Vitorge (France, 1994–1999); A. R. Ware (UK, 1998–1999); **National Representatives:** A. V. R. Reddy (India, 1996–1999); C. Testa (Italy, 1996–1999); I. S. Chang (Korea, 1998–1999); E. Steinnes (Norway, 1998–1999); A. Plonka (Poland, 1992–1999); J. M. Peixoto de Cabral (Portugal, 1992–1999); B. F. Myasoedov (Russia, 1986–1999); J. R. Gancedo Ruiz (Spain, 1992–1999); N. E. Holden (USA, 1986–1999).

Names of countries given after Members' names are in accordance with the *IUPAC Handbook 1998–1999*.

Republication or reproduction of this report or its storage and/or dissemination by electronic means is permitted without the need for formal IUPAC permission on condition that an acknowledgment, with full reference to the source, along with use of the copyright symbol ©, the name IUPAC, and the year of publication, are prominently visible. Publication of a translation into another language is subject to the additional condition of prior approval from the relevant IUPAC National Adhering Organization.

Critical evaluation of the chemical properties of the transactinide elements

(IUPAC Technical Report)

Abstract: In this paper, the chemical properties of the transactinide elements rutherfordium, Rf (element 104); dubnium, Db (element 105); and seaborgium, Sg (element 106) are critically reviewed. The experimental methods for performing rapid chemical separations on a time scale of seconds are reviewed, and comments are given on the special situation with the transactinides for which the chemistry has to be studied with single atoms. There follows a systematic description of theoretical predictions and experimental results on the chemistry of Rf, Db, and Sg—their mutual comparison and evaluation. The literature cited has the cutoff date of March 1999. The more recent chemical identification of bohrium, Bh (element 107), and of hassium, Hs (element 108), should be evaluated in a future Part II of this report.

CONTENTS

1. INTRODUCTION
 2. SYNTHESIS AND DECAY OF TRANSACTINIDES
 3. SINGLE-ATOM CHEMISTRY
 4. EXPERIMENTAL TECHNIQUES
 - 4.1 Target and transport systems
 - 4.2 Gas-phase chemistry
 - 4.3 Aqueous chemistry
 5. RUTHERFORDIUM (ELEMENT 104)
 - 5.1 Theoretical predictions
 - 5.2 Experimental results
 - 5.3 Evaluation
 6. DUBNIUM (ELEMENT 105)
 - 6.1 Theoretical predictions
 - 6.2 Experimental results
 - 6.3 Evaluation
 7. SEABORGIUM (ELEMENT 106)
 - 7.1 Theoretical predictions
 - 7.2 Experimental results
 - 7.3 Evaluation
 8. CONCLUSION
- ACKNOWLEDGMENTS
REFERENCES

1. INTRODUCTION

At this time, we know of 20 man-made transuranium elements. The first 11 artificial elements beyond uranium belong to the actinide series. Their chemistry is documented in a large number of review articles and books (e.g., [1–4]). According to the actinide concept [5], the 5f series ends with element 103, lawrencium (Lr), and a new 6d transition series is predicted to begin with element 104, rutherfordium

(Rf), see, e.g., [6]. Hence, the currently known 9 transactinide elements have been placed in the periodic table under their lighter homologs in the 5d series Hf, Ta, W, Re, Os, Ir, Pt, Au, and Hg. The peculiar arrangement of the first 5 actinides in some representations* of the periodic table with a shifted position with respect to the other actinides reflects the fact that, owing to a large delocalization of their 5f orbitals, the 5f electrons take part in their chemistry, a feature that is much less pronounced in the 4f series of the lanthanides. This makes Th a pseudohomolog of the group 4 elements Zr and Hf, Pa a pseudohomolog of the group 5 elements Nb and Ta, and, to a decreasing extent, U, Np, and Pu pseudohomologs of the groups 6–8 elements, respectively. The more uniform actinide behavior is found only for the second half of the actinides starting with Am.

Investigating the chemical properties of the transactinide elements is challenging both experimentally and theoretically. Owing to increasingly strong relativistic effects, increasing deviations from the periodicity of the chemical properties based on extrapolations from the lighter homologs in the periodic table have been predicted for some time [6]. They result from the increasingly strong Coulomb field of the highly charged atomic nucleus, which stabilizes the spherical s and $p_{1/2}$ orbitals. This, in turn, destabilizes and expands the d and f orbitals. Thus, electron configurations different from those known for the lighter homologs may occur as well as unusual oxidation states and radii. Relativistic quantum chemical calculations of molecules combined with fundamental physicochemical considerations of the interaction of these molecules with their chemical environment [7,8] now allow detailed predictions of the chemical properties of the heaviest elements and of those of their lighter homologs. Also, empirical extrapolations assuming linear regularities in the groups and periods of the periodic table are valuable to assess the significance of relativistic effects in the transactinides. However, these empirical extrapolations cannot be regarded as purely “nonrelativistic” because relativistic effects are present already in the lighter elements and increase down the groups in the periodic table. Thus, the experimenter’s approach will generally involve a detailed comparison of the chemical properties of the transactinides with those of their lighter homologs (and pseudohomologs) under identical conditions, as well as with the results of relativistic molecular orbital (MO) calculations in order to explore the role of relativistic effects in the heaviest elements.

If Rf** exhibits chemical properties similar to those of Zr and Hf, it should form volatile tetrachlorides. Thus, early experiments exploited the volatility of RfCl_4 in the gas phase [9–12]. In aqueous solutions, the complexing with α -hydroxyisobutyrate (α -HIB) [13] and the formation of anionic chloro-complexes [14] confirmed a behavior radically different from that of the heavy actinides. Although these were key experiments demonstrating that a new transition element series, the 6d series, begins with element 104, none of these experiments provided a detailed study of Rf chemistry. First-generation gas-phase experiments with chlorides [15] and bromides [16,17] of Db, element 105, indicated also for Db halides a much greater volatility than that of the respective actinide compounds. As the experimental deposition temperature in such thermochromatography experiments depends on the migration time and the latter, in turn, strongly depends on the nuclear half-life, these experiments [9–12,15–17] did not allow for detailed comparisons of the volatility of Rf and Db with the volatilities of their homologs. The respective correction technique based on a microscopic model of gas–solid interactions [18,19] in open columns was outlined later [17]. It was systematically applied in [20]. The results from the first-generation experiments on the chemistry of the transactinides were summarized in a number of review articles [21–24].

*See, e.g., the cover of the textbook *Fundamentals of Radiochemistry* by J.-P. Adloff and R. Guillaumont, CRC Press, Boca Raton (1993).

**In this article, the element names endorsed in 1997 by the International Union of Pure and Applied Chemistry are used. Note that the names kurtchatovium (Ku) and nielsbohrium (Ns) were used in some of the original publications of the Dubna group for elements 104 and 105. In publications of the Berkeley group and in earlier publications of the author, the name hahnium (Ha) for element 105 has been used.

A renewed interest in studying the chemical properties of the transactinide elements in more detail, both experimentally and theoretically, arose in the late 1980s; see [25–30] for recent reviews. This extensive series of detailed investigations was made possible by the development of new experimental techniques such as computer-controlled automated systems that have greatly improved our ability to perform rapidly and reproducibly large numbers of chromatographic separations on miniaturized columns in the liquid phase and to detect the transactinides through their characteristic α -decay and preferably by correlated $\alpha\alpha$ -mother–daughter correlations. Also, a vastly improved technique for gas-phase experiments coupled online to a versatile detection system for α -decay chains has been developed. Both techniques have produced detailed and sometimes surprising new results that called for a detailed theoretical modeling of the chemical species with improved quantum chemical codes.

In this review, the special conditions for the synthesis and decay of the transactinides are considered, followed by some remarks about performing chemistry with only one atom at a time. The experimental techniques are outlined, and a description of theoretical predictions and experimental results on the chemistry of Rf, Db, and Sg is given. Predictions and results are mutually compared and evaluated.

2. SYNTHESIS AND DECAY OF TRANSACTINIDES

Transactinides are being synthesized in nuclear fusion reactions with heavy-ion projectiles. Details of the production and decay of the heaviest elements are discussed in a number of reviews [31–39]. The production rates rapidly decrease from about 1 atom/min for element 104 to 1 atom per several days for the heaviest man-made elements. Half-lives decreasing from about 1 min to the order of magnitude of 1 ms for the longest-lived isotope of these elements present an additional challenge, especially for chemical investigations. Low production rates and short half-lives lead to the situation in which, on the average, each synthesized atom has decayed before a new one is made. The consequences for chemical studies with one atom at a time are discussed in the next section.

Cold fusion reactions in which ^{50}Ti , ^{54}Cr , ^{58}Fe , $^{62,64}\text{Ni}$, and ^{70}Zn projectiles are fused with ^{208}Pb and ^{209}Bi targets tend to give the highest possible cross-sections, however, the neutron-deficient product nuclei in these reactions have half-lives generally less than 1 s. This is too short for most existing chemical techniques, in particular for those that allow the study of detailed chemical properties. More neutron-rich and, hence, longer-lived products are obtained in hot fusion reactions of ^{18}O , ^{22}Ne , ^{26}Mg , and ^{34}S projectiles with actinide targets. Typical experimental conditions are heavy-ion beam currents of 3×10^{12} particles/s and a maximum useful target thickness of about $900 \mu\text{g cm}^{-2}$. Recent chemical studies of element 104 have used 78-s ^{261}Rf produced in the $^{248}\text{Cm}(^{18}\text{O}, 5\text{n})$ reaction with a cross-section of 5 nb. Recent studies of Db used 34-s ^{262}Db and 27-s ^{263}Db [40,41] produced in 5n- and 4n-reactions of ^{18}O with ^{249}Bk targets with cross-sections of 6 nb and 2 nb, respectively. These conditions yield production rates of 1 atom/min or less. Thus, all chemical studies with transactinide elements are truly performed with single atoms.

The discovery of the neutron-rich isotopes ^{265}Sg and ^{266}Sg [42] of element 106, seaborgium (Sg), with half-lives estimated on the basis of α -energy systematics to be on the order of 2–30 s and production cross-sections of 260 pb and 60 pb in the $^{248}\text{Cm}(^{22}\text{Ne}, 5\text{n})$ - and $^{248}\text{Cm}(^{22}\text{Ne}, 4\text{n})$ -reactions, respectively, has paved the way for chemical studies of Sg [43]. (The non-SI unit barn, symbol b, is defined as 10^{-24}cm^2 ; thus $1 \text{pb} = 10^{-36} \text{cm}^2$.)

Nuclides with half-lives presumably sufficiently long to explore the chemistry of element 107, bohrium (Bh), ^{267}Bh and ^{266}Bh , can be produced in the $^{22}\text{Ne} + ^{249}\text{Bk}$ reaction. For element 108, hassium (Hs), ^{269}Hs with a half-life of 10 s [44] will be used for chemical studies. A suitable production reaction is $^{26}\text{Mg} + ^{248}\text{Cm}$. These long half-lives are due to the enhanced nuclear stability near the deformed shell $N = 162$.

3. SINGLE-ATOM CHEMISTRY

For a chemical reaction



the Gibbs energy of reaction is

$$\Delta G = \Delta G^\circ + RT \ln \frac{a^x(X) \cdot a^z(Z)}{a^b(B) \cdot a^e(E)}, \quad (2)$$

where a are activities (or in less rigorous treatments concentrations, partial pressures) of the substances involved. According to the law of mass action,

$$\frac{a^x(X) \cdot a^z(Z)}{a^b(B) \cdot a^e(E)} = K, \quad (3)$$

where K is the equilibrium constant. For equilibrium, $\Delta G = 0$, and

$$\Delta G^\circ = -RT \ln K. \quad (4)$$

This is well established for macroscopic quantities where, e.g., metal ions M are constituents of B and X at the same time, and eq. 1 characterizes a dynamical, reversible process in which reactants and products are continuously transformed into each other back and forth even at equilibrium. If only one atom of M is present, it cannot be a constituent of B and X at the same time and at least one of the activities on the left- or right-hand side of eq. 1 is zero. Consequently, an equilibrium constant can no longer be defined, and the same holds for the thermodynamic function ΔG_0 . Does it make sense, then, to study chemical equilibria with a single atom?

Guillaumont et al. [45,46], in view of this dilemma, have pointed out that chemical speciation of nuclides at the tracer scale is usually feasible with partition methods in which the species to be characterized is distributed between two phases. This can be an aqueous and an organic phase or a solid and a gas phase. According to [45], single-atom chemistry requires the introduction of a specific thermodynamic function, the single-particle free energy. An expression equivalent to the law of mass action is derived in [45] in which activities (concentrations or partial pressures) are replaced by the probability of finding the species in the appropriate phase. According to this law, an equilibrium constant (i.e., the distribution coefficient K_d of M between two phases) is correctly defined in terms of the probabilities of finding M in one phase or the other. If a static partition method is used, this coefficient must be measured many times in repetitive experiments. Since dynamical partition methods (chromatographic separations) can be considered as spatially repetitive static partitions, the displacement of M along the chromatographic column, in itself, is a statistical result and only one experiment is necessary, in principle. This underlines the validity of partition experiments with single atoms and the particular attraction of chromatographic methods in single-atom chemistry.

For short-lived atoms, additional considerations with regard to the kinetics are in order. The partition equilibrium must be reached during the lifetime of the atom, which requires high reaction velocities. Let us consider a single-step exchange reaction



Here, M is a single atom that can bind with either X or Y ; k_5 and k_{-5} are the rate constants for the forward and backward reactions. The rate of a chemical reaction depends on the height of the reaction barrier between the states $MX + Y$ and $MY + X$, because in-between, there is a state of high potential energy—the transition state $[Y...M...X]$.

This state is unstable because the old chemical bond is not completely disrupted and the new one not yet completely formed. If the Gibbs energies of activation $\Delta^\ddagger G_5$ and $\Delta^\ddagger G_{-5}$ for the reactions forth

and back are high, the reaction proceeds very slowly. The transitions from left to right and from right to left do not occur with sufficient frequency, and the system is far from its thermodynamical equilibrium. Borg and Dienes [47] found that, only if $\Delta^\ddagger G$ is less than 15 kcal (60 kJ), will the residence time of M in each state MX or MY be short (<1 s). Then, an equilibrium is rapidly reached (in times short compared with the nuclear half-lives of the transactinides). Borg and Dienes point out that the average time that M spends as MX or MY is proportional to the equilibrium constant. Thus, a measurement of the partition of M between the states MX and MY with very few atoms of M will already yield an equilibrium constant close to the "true" value provided that both states are rapidly sampled. This tells us again that chromatographic systems with fast kinetics are ideally suited for single-atom separations as there is rapid, multiple sampling of the absorbed or mobile species. The fractional average time that M spends as the absorbed species (which is proportional to the equilibrium constant, see above) is closely related to the chromatographic observable, the retention time.

4. EXPERIMENTAL TECHNIQUES

Recent reviews of fast chemical separation procedures developed for transactinide studies can be found in [30,48]. Nevertheless, the most pertinent techniques are also presented here.

4.1 Target and transport systems

A typical target-and-recoil chamber arrangement is as follows. Heavy-ion beams pass through a vacuum isolation window, a volume of nitrogen cooling gas, and a target backing before interacting with the target material. Reaction products recoiling out of the target are thermalized in a volume of He gas loaded with aerosol particles of 10–200 nm size to which the reaction products attach. At a flow rate of about 2 l min⁻¹, the transport gas with the aerosols is transported through capillary tubes (~1.5-mm inner diameter) to the chemistry apparatus where it deposits the reaction products. He/aerosol-jets allow for transportation over distances of several tens of meters with yields of about 50 % [49–52]. Transport times are on the order of 2–5 s. Aerosol materials are selected to minimize their influence on the chemical procedures. Separations in the aqueous phase often use KCl [49,50,52] as aerosol, while MoO₃ and carbon clusters have been preferred in gas-phase separations [51].

In the early frontal gas-chromatographic experiments with element 104 [10,11], the target-and-recoil chamber was bombarded by the internal beam inside the cyclotron. The recoils were stopped in nitrogen heated to 300 °C (flow rate 18–20 l min⁻¹) and transported into an outlet tube (i.d. 3.5 mm) at a distance of 3 cm from the target, where a stream of nitrogen (0.5–1.0 l min⁻¹) containing the reactive chlorinating gases NbCl₅ and ZrCl₄ was introduced. The volatile RfCl₄ was transported through the 4-m-long outlet tube to mica fission-track detectors outside of the cyclotron. Later, the external beam of the cyclotron was used with the chromatography columns coupled directly to the target-and-recoil chamber [12,15,16,53–57]. In this configuration, typically 60 % of the recoils reach the column without the use of aerosols. Transport times of <1 s were measured [54]. The disadvantage of this direct coupling was that the detection of the transactinides had to be performed in a hostile chemical environment so that detection of α -particles with semiconductor detectors was not possible and the detection was limited to the unspecific spontaneous fission (SF) by solid-state track detectors.

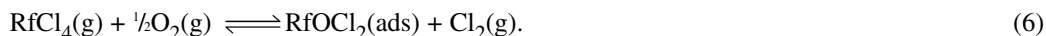
4.2 Gas-phase chemistry

One of the distinctive chemical properties of the groups 4–6 elements is that they form volatile halides and oxohalides. Thus, the volatility of these compounds can be used for a separation of these elements via the gas phase.

Vapor pressure curves of the monomeric gas over the respective solids [20,58,68] provide a measure of the volatility of compounds. These curves are calculated using tabulated standard sublimation

enthalpies, $\Delta_{\text{sub}}H^\circ$, and standard sublimation entropies, $\Delta_{\text{sub}}S^\circ$ [59]. They show that HfCl_4 and HfBr_4 are slightly more volatile than the Zr homologs, but less volatile than TaCl_5 and NbCl_5 .

It is interesting to note that the chlorides and bromides of Zr and Hf show similar volatilities, whereas NbBr_5 and TaBr_5 are considerably less volatile than the respective pentachlorides. The existence in the gas phase of ZrOCl_2 and HfOCl_2 is uncertain. Morozov et al. [60] found that ZrOCl_2 and HfOCl_2 decompose to the tetrachloride and the oxide when heated and determined the vapor pressure curves of the tetrachlorides over their oxochlorides. Domanov et al. [61] observed that the deposition temperature for Zr and Hf depends on the O_2 concentration in the reactive gas. Based on these observations, Eichler [62] suggested a transport reaction mechanism ("reaction gas chromatography") with the tetrachloride in the gas phase and the oxochloride as the adsorbed state, i.e.,



Jost et al. [63] presented experimental evidence for this transport reaction mechanism.

Because only single molecules can be studied in experiments with transactinide elements, $\Delta_{\text{sub}}H^\circ$, of RfCl_4 , for example, cannot be determined directly. The quantity deduced from gas chromatography experiments is $\Delta_{\text{ads}}H^\circ$, the adsorption enthalpy at zero coverage on the chromatographic surface (usually quartz). As was demonstrated by Zvara et al. [53], a linear correlation exists between $\Delta_{\text{ads}}H^\circ$ and $\Delta_{\text{sub}}H^\circ$ for chlorides. By measuring $\Delta_{\text{ads}}H^\circ$ of chlorides of 24 elements on quartz surfaces, Eichler et al. [64] established the empirical relation

$$-\Delta_{\text{ads}}H^\circ = (0.655 \pm 0.042) \text{ kJ/mol} \cdot \Delta_{\text{sub}}H^\circ + (18.0 \pm 8.8) \text{ kJ/mol} \quad (7)$$

Thus, $\Delta_{\text{ads}}H^\circ$ is the quantity used to judge the volatility of the transactinide compounds relative to the volatility of their lighter homologs, which are also studied in weightless amounts (i.e., at zero coverage).

There are two experimental approaches to determine $\Delta_{\text{ads}}H^\circ$ —thermochromatography and isothermal gas chromatography. In thermochromatography [12,15–19,53–57], a longitudinal, negative temperature gradient is established along the chromatography column in the flow direction of the carrier gas. Volatile species are deposited in the column according to their volatility and form distinct deposition zones. Mica sheets, or glass, quartz or polymer plates, inserted into the chromatography column serve as fission track detectors. The method has the advantage of a very high speed at which the production of volatile species and their separation occurs. The recoiling reaction products are rapidly swept from the target chamber to the entrance of the chromatography column where halogenating reactive gases are added. Transactinides decaying by SF are registered in the column at a characteristic deposition temperature, thus providing information about their volatility. These experiments are simple and relatively easy to perform. However, thermochromatography also shows serious disadvantages. The fact that the position of the deposition zones of homologs can be measured only after completion of the experiment makes the interpretation of the relative volatility of the short-lived transactinides, compared to the detected much longer-lived homologs, difficult. In addition, real-time detection of the nuclear decay of transactinides and the determination of their half-lives is not possible. Moreover, SF is an unspecific decay mode of many actinides and transactinides, which allows no identification of the atomic number nor of the decaying nuclide.

In order to overcome these serious disadvantages, online isothermal gas chromatography was developed and was successfully applied to study the volatility of Rf, Db, and Sg halides and oxohalides [20,58,63,65–69,103,105]. The most advanced apparatus is the online gas chemistry apparatus (OLGA III), coupled to the rotating multidetector apparatus (ROMA).

The reaction products, attached to graphite aerosols, are continuously transported through a capillary to the OLGA set-up. In the first section of the chromatography column, the aerosols are stopped on a quartz wool plug. This section is heated to 900–1000 °C. At the position of the quartz wool plug, reactive gases such as HBr, BBr_3 , HCl, Cl_2 , SOCl_2 , and O_2 are added at typically 100–300 ml/min. The second part of the quartz column serves as an isothermal chromatography section. It has a length of 2 m,

a diameter of 1.5–2 mm, and has temperature gradient from room temperature to 500 °C. Volatile species pass through this section where they undergo numerous sorption/desorption steps with retention times indicative of the volatility at the given temperature of the isothermal part of the column. The chemical yield of the volatile species is studied as a function of the temperature of the isothermal part of the column. The chemical yield rises steeply above a certain temperature and reaches a plateau at higher temperatures. The retention time of the volatile species is determined by using the nuclear half-life of the radionuclides as a “clock”: At the temperature at which 50 % of the plateau yield is observed, $T_{50\%}$, the retention time is equal to one half-life. To measure the decay of the separated species they are, after exiting the chromatographic column into a water-cooled “recluster chamber”, attached to new aerosols and transported through a capillary to a detection system, a rotating wheel such as ROMA or a moving tape system [20] that positions the deposited activity in front of successive passivated ion-implanted planar silicon (PIPS) detectors which register α -particles and SF events. The energies of the events are stored in list mode with the time and detector designation for offline processing of the data. This allows searching for time-correlated parent–daughter pairs of α -events, or even longer α -decay chains, as well as α -SF correlations; in certain cases, this provides an unambiguous identification of single events.

Based on Zvara’s microscopic model of gas–solid thermochromatography in open columns [18], a Monte Carlo code was made available [20] that allows generation of thermochromatographic deposition zones as well as yield-vs.-temperature curves as observed in isothermal chromatography. This model accommodates the influence of the carrier gas flow, the actual temperature profiles, and the different half-lives of the investigated species. For each isothermal temperature, the transport through the column is modeled for a large number of sample molecules. These calculations result in a curve of yield-vs.-temperature for each value of the adsorption enthalpy $\Delta_{\text{ads}}H^\circ$. The curve for the particular $\Delta_{\text{ads}}H^\circ$ that best fits the measured data is chosen by a least-squares method. In the correlation of the retention time with $\Delta_{\text{ads}}H^\circ$, the adsorption entropy $\Delta_{\text{ads}}S^\circ$ according to the formalism of Eichler and Zvara [70] is used.

4.3 Aqueous chemistry

While gas-phase chemistry is carried out continuously as an online process, aqueous chemistry has been performed mostly in a discontinuous, batch-wise manner. It is then necessary, in order to get a statistically significant result, to repeat the same experiment several hundred or even several thousand times with a cycle time of typically 1 min. Recent discontinuous studies were either performed manually [71–76] or with the automated rapid chemistry apparatus, ARCA II [40,41,43,77–83].

One of the manual separations made use of the characteristic adsorption of the group 5 elements Nb, Ta, and Db from nitric acid on glass surfaces [71]. Another used thin film ferrocyanide surfaces for the study of the hydrolysis of Rf [74]. All other manual separations were liquid–liquid extractions typically comprising the following steps: the KCl aerosol with the reaction products was collected on a platinum or Teflon™ slip for 60–90 s, picked up with 10 μl of the aqueous phase, and transferred to a 1-ml centrifuge cone containing 20 μl of the organic phase. The phases were mixed ultrasonically for 5 s and centrifuged for 10 s for phase separation. The organic phase was transferred to a glass cover slip, evaporated to dryness on a hot plate, and placed over a PIPS detector. This procedure took about 1 min and was mainly applied to study the aqueous chemistry of Rf with 78-s ^{261}Rf [72,73,75,76]. Surprisingly, the aqueous phase was not counted.

Automated separations with ARCA II were performed with Rf [80,83], Db [40,41,77–79,81], and Sg [43,82]. ARCA II is a computer-controlled apparatus for fast, repetitive high-performance liquid chromatography (HPLC) separations [84].

ARCA II consists of a central catcher-chemistry part incorporating horizontally movable sliders, and two movable magazines containing 20 of the chromatographic columns (1.6 \times 8 mm) each, and peripheral components (i.e., three chemically inert HPLC pumps) and a number of pneumatically driven

four-way slider valves. Each pump is dedicated to one eluent. In the case of separations of Db in mixed HCl/HF solutions [77], one pumps 12 M HCl/0.02 M HF, the second 4 M HCl/0.02 M HF, and the third 6 M HNO₃/0.015 M HF through Teflon tubing of 0.3-mm inner diameter to the central catcher-chemistry unit. The He(KCl) gas jet deposits the transported reaction products continuously onto one of two frits. After 1 min collection, the frit is moved on top of one of the microcolumns, washed with 12 M HCl/0.02 M HF, whereby the reaction products are dissolved, complexed, and extracted into the organic phase (the columns are filled with Teflon grains coated with tri-isooctyl amine, TiOA), while the nonextractable species (notably the actinides) run through into the waste. The column is then washed with 4 M HCl/0.02 M HF, and the effluent (containing Nb, Pa, and Db) is directed to the fraction collector where it is collected on a Ta disk and quickly evaporated to dryness by intense infrared light and hot He gas. Next, the Ta fraction is eluted with 6 M HNO₃/0.015 M HF, collected on a Ta disk, and evaporated to dryness. The Ta disks are inserted into the counting chambers about 55 s after the end of collection. Five seconds later, the next 1 min collection on the twin frit is complete. That frit is moved on top of the second column contained in the opposite magazine, and the next separation cycle is carried out. After each separation, the magazine is moved by one step, thus introducing a new column into the elution position. In this way, the time-consuming reconditioning of used columns and cross-contamination from previous separations is avoided. After 40 min of continuous collection and separation cycles, the program is stopped. The used magazines are removed, two new magazines are introduced, and another 40 cycles are started. More than 7800 of such and similar ARCA II experiments have been conducted in the study of Db so far.

Recently, continuous isolation procedures have been developed, the first of these for nuclear decay studies of Hf, Ta, and W isotopes [85], which was subsequently applied to Rf [86] in combination with a discontinuous sample preparation step.

Reaction products transported by an aerosol jet were continuously dissolved in the aqueous phase, which was pumped through three consecutive ion-exchange columns. Trivalent actinides were retained on the first cation-exchange column followed by an anion-exchange column to adsorb anionic fluoride complexes of element 104, and a third column filled with a cation-exchange resin to collect the trivalent daughter products from the α -decay of ²⁶¹Rf. At the end of an experiment, the ²⁶¹Rf daughter products, 3.0-d ²⁵³Fm and 20-d ²⁵³Es, were stripped from this third column to prepare a sample for offline α -spectroscopy. The detection of ²⁵³Es in that sample was proof that ²⁶¹Rf had formed anionic fluoride complexes that had been retained on the anion-exchange column.

Pfrepper et al. [87,88] have developed this method further, thereby making it a quantitative technique capable of measuring distribution coefficients K_d . In the conventional offline chromatography as performed by ARCA II, the distribution coefficient is determined via the retention time (elution position) as

$$K_d = (t_r - t_o) \frac{V}{M} \quad (8)$$

with t_r = retention time,
 t_o = column hold-up time due to the free column volume,
 V = flow rate of the mobile phase (ml min⁻¹), and
 M = mass of the ion exchanger (g).

As in [86], the detection of the transactinide isotope itself, ²⁶¹Rf, is abandoned and replaced by the detection of its long-lived descendant, 20-d ²⁵³Es. In this way, one gains the possibility of a continuous online mode over many hours. The feeding of ²⁶¹Rf onto the anion-exchange column is performed under conditions in which the retention time t_r is on the order of the nuclear half-life $t_{1/2}$ (i.e., K_d values on the order of 10–50 are selected) [87]. Similar to the principle used in online isothermal gas chromatography, the nuclear half-life is used as an internal clock. As in [86], three ion-exchange columns are used in series, first a cation-exchange column that retains the ²⁵³Es from the continuously flowing feed solution. This is necessary as ²⁵³Es can be produced directly by transfer reactions. The next is the true chro-

matographic column filled with an anion-exchange resin. The long-lived decay products $N(D_1)$ that are formed by radioactive decay of ^{261}Rf during its retention time on the anion-exchange column are eluted from this column as cations and are fixed on the following cation-exchange column. The part of the ^{261}Rf that survives the retention time on the anion-exchange column is eluted from it and passes the following cation-exchange column to be subsequently collected in a reservoir in which it decays into the long-lived decay products $N(D_2)$. $N(D_1)$ and $N(D_2)$ are isolated separately after the end of the online experiment and assayed offline for α -activity of ^{253}Es . From the ratio of $N(D_1)$ and $N(D_2)$ and the nuclear half-life of ^{261}Rf , one obtains the distribution coefficient

$$K_d = \left[\frac{t_{1/2}}{\ln 2} \ln \frac{N(D_1) + N(D_2)}{N(D_2)} - t_0 \right] \frac{V}{M}. \quad (9)$$

This principle has been applied to Rf in fluoride solutions [88].

The centrifuge system SISAK III [89] allows a continuous separation of nuclides with half-lives down to 1 s. The separation is based on multistage liquid–liquid extractions using static mixers and specially designed mini-centrifuges for subsequent phase separation. SISAK was successfully applied to a large number of γ -spectroscopic studies of lighter elements. Recently, a new detection system based on liquid scintillation spectroscopy was developed for online α -spectroscopy and SF detection in the flowing organic phase from SISAK [90]. Between α -energies of 4.8 and 7.4 MeV, energy resolutions of 210 through 330 keV are achieved. Suppression of interfering β - and γ -radiation is obtained by pulse-shape discrimination and pile-up rejection. An online model experiment for element 104 was carried out [90] using the α -emitter 17-s ^{161}Hf . However, in experiments with ^{261}Rf , due to a high level of interfering β - and γ -radiation, the number of random $\alpha\alpha$ -mother–daughter correlations due to pile-up was too large to allow for an unambiguous identification of ^{261}Rf decay chains. Work is going on to improve the pulse-shape discrimination and pile-up rejection.

5. RUTHERFORDIUM (ELEMENT 104)

5.1 Theoretical predictions

From extrapolation of the ground-state electron configurations of Ti, Zr, and Hf, Rf would be expected to have the configuration $[\text{Rn}]5f^{14}6d^27s^2$. This configuration was also indicated by early relativistic calculations [91,92] in a Dirac–Fock computer code with a single configuration approximation.

After multiconfiguration Dirac–Fock (MCDF) calculations had indicated that, because of the relativistic stabilization of the $p_{1/2}$ orbital, the electronic structure of Lr is $[\text{Rn}]5f^{14}7s^27p_{1/2}$, rather than $[\text{Rn}]5f^{14}6d7s^2$ [93,94], it was extrapolated that Rf should have a $7s^2p^2$ rather than a $6d^27s^2$ configuration [23]. This raised the question whether Rf might be a “p-element” with properties similar to Pb, which has a ground-state configuration $[\text{Xe}]4f^{14}5d^{10}6s^2p^2$. However, it should be noted that, contrary to Rf, Pb has a closed 5d shell and a large energy gap of more than 4 eV between its ground state and the next higher state.

A more recent MCDF calculation using 468 jj-configurations gave an (80 %) $6d7s^27p$ ground-state configuration for Rf [95] with the $6d^27s^2$ level (95 %) only 0.5 eV higher. This calculation predicted the $7s^27p^2$ state to be 2.9 eV above the ground state. The $6d7s^27p$ ground-state configuration was confirmed in a similar MCDF calculation [96] with an energy gap of only 0.24 eV to the next higher state.

Relativistic coupled-cluster calculations, based on the Dirac–Coulomb–Breit Hamiltonian (CCSD) including dynamical correlations [97], reverted to the $6d^27s^2$ configuration as the ground state of Rf, but the $6d7s^27p$ state is only 0.274 eV above the ground state.

From MCDF calculations, ionization potentials, atomic radii, and ionic radii were deduced [96,98]. It was found that radii, orbital energies, and ground levels of ionized states of Rf are similar to Hf and much different from Pb [98] so that it was concluded that there is no solid basis for expecting a

“p-character” for Rf and that its basic properties will resemble those of Zr and Hf. From a relativistic density-functional computation (SCF- $X\alpha$ scattering wave) for RfCl_4 , a lower effective charge of the central metal ion and a higher covalency in the metal–chloride bonds was obtained [98]. This should give rise to a higher volatility of RfCl_4 compared to that of ZrCl_4 and HfCl_4 .

Quantum chemical calculations using the Dirac–Slater discrete variational method (DS DVM) were performed to study the electronic structure of the group 4 tetrachlorides and of PbCl_4 [99] and of the highest chlorides of the groups 4–6 elements [100]. These calculations agree that the electronic structures of RfCl_4 and HfCl_4 are similar and that the bonding is typical of a d-element compound. Both calculations also show [99,100] that RfCl_4 is a rather covalent compound, more covalent than HfCl_4 . A stronger metal–ligand bond in RfCl_4 should make RfCl_4 thermally more stable than ZrCl_4 and HfCl_4 [100].

5.2 Experimental results

The pioneering experiments with Rf in the gas phase [9–12] demonstrated that Rf forms volatile chlorides and that RfCl_4 is much more volatile than the actinide chlorides and similar to HfCl_4 . Originally, the authors claimed [10] that the spatial distribution of fission tracks was compatible with the half-life of 0.3 s that they believed to be associated with the isotope ^{260}Rf . It was also claimed that the volatility of RfCl_4 was somewhat less than that of HfCl_4 [10]. These claims in [10] are evidently incorrect. Firstly, an isotope of Rf with a half-life of 0.3 s has never existed [101], and secondly, it is impossible to determine both the half-life and the heat of adsorption from a fission track distribution. Later, Zvara et al. [54] reinterpreted their original experiments by considering “the possible chromatographic effect of retention” and suggested that they were evidently dealing with 3-s ^{259}Rf , an α -emitter discovered earlier at Berkeley [102]. There is ongoing discussion about the existence of a fission branch in this isotope. The thermochromatographically determined deposition zones for spontaneously fissioning isotopes in [54] were close to the distribution of $^{170,171}\text{Hf}$, meaning that Rf and Hf tetrachlorides have similar volatilities.

In [53], a strongly enhanced retention of the RfCl_4 is reported when KCl is provided as the solid phase instead of glass, most likely due to the formation of nonvolatile K_2RfCl_6 .

A careful discussion of the results of online isothermal gas chromatography experiments with the group 4 elements Zr, Hf, and Rf, is given in [20]. We refer here to the most recent results by Kadkhodayan et al. [103] using HEVI. In these experiments, a MoO_3 aerosol gas jet was used to transport the activities from the recoil chamber to the chromatography apparatus. The MoO_3 after reaction with chlorinating reagents forms volatile oxochlorides that do not deposit inside the chromatography column. A total of 837 α -particles attributed to the decay of ^{261}Rf and its daughter ^{257}No were detected after the gas-phase separation, including 170 $\alpha\alpha$ -correlations. A half-life of 78_{-6}^{+11} s resulted from the decay of ^{261}Rf , in good agreement with the 65 ± 10 s literature value [104].

The experimental data were analyzed with the Monte Carlo model mentioned in Section 4.2 to yield adsorption enthalpies $\Delta_{\text{ads}}H^\circ$ for group 4 chlorides on SiO_2 surfaces, which are -74 ± 5 kJ/mol for Zr, -96 ± 5 kJ/mol for Hf, and -77 ± 6 kJ/mol for Rf. It should be noted that the fits of the Monte Carlo curves to the data are rather poor such that the uncertainties given may be unrealistic. Note also, that the values of adsorption enthalpies deduced from the Monte Carlo simulations are based on a number of assumptions, i.e., the adsorption enthalpy does not depend on temperature and on the composition of the carrier gas, and the adsorption entropy is known *a priori* [70]. The lower volatility of Hf chloride, if significant, is surprising in view of the known vapor pressure curves, as the experimental conditions were kept as similar as possible to the ZrCl_4 - and RfCl_4 -experiments [103]. It is not clear whether Hf is more susceptible to trace impurities in the system (O_2 , H_2O), thus forming HfOCl_2 in the adsorbed state, eq. 6. This would shift the yield-vs.-temperature curve to higher temperatures.

Within the error limits, RfCl_4 exhibits about the same volatility as ZrCl_4 and thus shows the volatility expected from relativistic calculations [100]. From “nonrelativistic” extrapolations one would

expect a less volatile RfCl_4 . Further experiments under absolutely oxygen-free conditions, and with a higher resolution with respect to the determination of the observable $T_{50\%}$, are desirable before quantitative conclusions on the influence of relativistic effects on the volatility of RfCl_4 can be drawn.

The volatility of short-lived Hf and Rf in chlorinating, oxygen-containing gases was investigated recently by Jost et al. [63], 150 ml/min Cl_2 , saturated with thionyl chloride (SOCl_2) and 20 ml/min O_2 were used as reactive gases. The 50 % temperature for Hf was found to be shifted to 390 °C, whereas for a simple adsorption/desorption process of HfCl_4 , $T_{50\%}$ would be expected at ~200 °C. For Rf, the yield-vs.-temperature curves were compared for the reactive gases (i) 300 ml/min HCl and (ii) 150 ml/min Cl_2 saturated with SOCl_2 , 20 ml/min O_2 .

A shift of the $T_{50\%}$ value from about 125 °C to about 330 °C is observed with a much slower increase of the yield in the presence of oxygen. This is strong evidence for the proposed transport reaction, eq. 6. A modification of the Monte Carlo model to take care of the different transport reaction mechanism ("reaction gas chromatography") will be discussed in Section 7. The Rf data for HCl as chlorinating agent in [63] are in agreement with those in [103].

In [65], a higher volatility for Rf bromides than for the lighter Hf homologs was reported for the first time. More recent data [105] allow comparison of the volatility of RfCl_4 with that of RfBr_4 , which turns out to be less volatile. The yield-vs.-temperature curve of the latter shifted to higher temperatures by about 150 °C. It is interesting to note that, in these experiments, the simultaneously measured behavior of Hf indicated a lower volatility of both the chloride and the bromide compared with the corresponding Rf chloride and bromide, respectively.

One experiment in the gas phase was carried out to probe a possible p-element behavior of Rf in its atomic state [106]. p-Elements such as Tl, Pb, and Bi in the elemental state show a much higher volatility than the group 4 elements Ti, Zr, and Hf. By analogy to a similar experiment on Lr [107,108], the retention of Rf in a quartz column at 1170 °C was measured in hydrogen containing Ar carrier gas. All fission tracks from 2.6-h ^{256}Fm , an unwanted by-product produced in the nuclear reaction, and from 3-s ^{259}Rf were observed in the region of the column where d-elements deposit. A lower limit for the sublimation enthalpy of $\Delta_{\text{sub}}H^\circ(\text{Rf}) \geq 370$ kJ/mol was determined. This result is in agreement with predictions [98,99] saying that, despite a possible $6d7s^27p$ ground-state configuration, in the interaction with any chemical environment Rf will behave similarly to Hf.

The first aqueous-phase separations of Rf [13] were performed with a cation-exchange chromatography column and the chelating reagent α -HIB. Rf was eluted together with Zr and Hf from the column while the trivalent actinides were strongly retained on the column. The chloride complexation of Rf was investigated in an automated solvent extraction chromatography experiment with the quaternary ammonium chloride Aliquat 336 on an inert support as stationary phase and 12 M HCl as the mobile phase [14]. Under these conditions, Zr, Hf, and Rf were extracted into the amine while the trivalent actinides were not retained on the column. The Rf, together with the Hf tracer, was then eluted in 6 M HCl. Although only 6 α -decays of ^{261}Rf were detected, this experiment demonstrated that the chloride complexation of Rf is similar to that of Hf and much stronger than that of the actinides [14].

A series of manually performed separations of ^{261}Rf from aqueous solutions was performed by the Berkeley group [72–76]. Liquid–liquid extractions with TiOA from 12 M HCl [72] confirmed the results of [14]. Cationic species were investigated by extraction into thenoyltrifluoroacetone (TTA). A distribution coefficient for Rf between those of the tetravalent pseudo homologs Th and Pu indicated [109] that the hydrolysis of Rf is less than that for Zr, Hf, and Pu.

Czerwinski et al. [73] performed a series of liquid–liquid extractions with tributyl phosphate, (TBP), in benzene to study the effect of HCl, Cl^- and H^+ ion concentration between 8 and 12 M on the extraction of Zr^{4+} , Hf^{4+} , Th^{4+} , Pu^{4+} , and Rf^{4+} . It was found [73] that Rf (like Zr, Th, and Pu) extracts efficiently as the neutral tetrachloride into TBP from 12 M HCl, while the extraction of Hf was relatively low and increased from 20 to 60 % between 8 and 12 M HCl. Extraction of Rf increased from 60 to 100 % between 8 and 12 M HCl, thus defining an extraction sequence $\text{Zr} > \text{Rf} > \text{Hf}$ for the group 4

chlorides. Surprising results were obtained when the chloride concentration was varied at a constant H^+ concentration of 8 M. Above 10 M Cl^- concentration, the extraction of Rf decreased and behaved differently from Zr, Hf, and Th, and resembled that of Pu^{4+} . This was interpreted in terms of stronger chloride complexing in Rf than in Zr, Hf, and Th, leading to the formation of $RfCl_6^{2-}$ [25], which is not extracted into TBP. Extraction studies at a constant concentration of 12 M Cl^- showed that Rf extraction increases sharply with increasing H^+ -concentration between 8 and 12 M [73]. Such behavior is not exhibited by Zr and Hf. As some of these extraction experiments suffered from differences in the details of the chemical procedures applied to the different elements, (e.g., different contact times and volumes used), it is important to confirm these very interesting findings in an experiment that establishes identical conditions for all homologous elements, including Rf.

Kacher et al. [75] performed some additional chloride extractions into TBP/benzene with Zr, Hf, and Ti. The low extraction yields of Hf by Czerwinski et al. [73] could not be reproduced by Kacher et al. [75], who reported that significant amounts of Hf (more than 50 % in some cases) stuck to the Teflon surfaces. (They actually conducted their subsequent experiments with polypropylene equipment because only negligible adsorption was observed with polypropylene surfaces.) The Hf results from the Czerwinski et al. experiments [73] were based on online data taken at the cyclotron where the activity was collected on a Teflon disk, which according to [75] accounts for the seemingly low Hf extraction. Surprisingly, a similar loss of Rf due to adsorption in the Czerwinski et al. work [73] was not suspected by Kacher et al., and so the latter authors, based on their new Zr, Hf, and Ti results and on the old [73] Rf results, suggested a revised sequence of extraction into TBP/benzene from ca. 8 M HCl as $Zr > Hf > Rf > Ti$. In a parallel study of liquid–liquid extractions into TBP/benzene from HBr solutions, extraction of Rf was found to be low and was only increased for bromide concentrations beyond 9 M [75].

The extraction behavior of the group 4 elements into TBP from both HCl and HBr solutions was primarily attributed to their different tendencies to hydrolyze [75]. The latter statement refers to concurrent work by Bilewicz et al. [74] who studied the sorption of Zr, Hf, Th, and Rf on cobalt ferrocyanide surfaces. These ferrocyanides are known to be selective sorbents for heavy univalent cations such as Fr^+ , Cs^+ , and Rb^+ . However, some ferrocyanides, such as Co ferrocyanide, have been found to exhibit also particularly high affinities for tetravalent elements such as Zr^{4+} , Hf^{4+} , and Th^{4+} involving the formation of a new ferrocyanide phase between the 4^+ cation and the $Fe(CN)_6^{4-}$ anion.

The hydrolysis of a 4^+ cation is shown in the following reaction



On the left-hand side of eq. 10, we have the hydrated 4^+ cation, on the right-hand side the first hydrolysis product, being a 3^+ cation.

As 3^+ cations are essentially not sorbed by ferrocyanide surfaces, the onset of hydrolysis at decreasing HCl concentration in the aqueous phase will be reflected by a rapid decrease of the sorbed activity. This decrease was observed by Bilewicz et al. [74] below 3 M HCl for Rf, below 1 M HCl for Zr, and below 0.5 M HCl for Hf, establishing seemingly a hydrolysis sequence $Rf > Zr > Hf$. As hydrolysis increases with decreasing radius of the cation, the stronger hydrolysis of Rf is very surprising and in conflict with the results in [109]. Bilewicz et al. suggested as an explanation that the predominant coordination number N_c (x in eq. 10) for Zr^{4+} and Hf^{4+} is 8, and changes to $N_c = 6$ for Rf due to relativistic effects making the $6d_{5/2}$ orbitals unavailable for ligand bonding of water molecules. Günther et al. [80] have shown that this does not withstand a critical examination. It is the author's opinion that some experimental problem and not the increased tendency of Rf to hydrolyze produced the surprising results [74]. For example, the contact time of the aqueous phase with the ferrocyanide surface was only 10 s in the Rf experiments. In a kinetic study, the authors found that Zr and Hf sorbed within 20 and 40 s, respectively, while Th required more than 90 s to achieve nearly complete sorption [74]. It is conceivable that, within the 10 s interaction of the aqueous phase in the Rf experiments, no equilibrium was established, thus making the Rf data meaningless.

A study of the extraction of fluoride complexes of Ti^{4+} , Zr^{4+} , Hf^{4+} , and Rf^{4+} into TiOA was also reported by Kacher et al. [76]. This work presents some evidence for extraction of ^{261}Rf into TiOA from 0.5 M HF. However, no quantitative assessment of the extraction yield or K_d value is made, so the conclusion in [76] that the extraction into TiOA for the group 4 elements decreases in the order $\text{Ti} > \text{Zr} \approx \text{Hf} > \text{Rf}$ is not tenable.

In view of the somewhat unsatisfactory situation with the conflicting Hf results in [73,75] and with the intention to establish an independent set of data characterizing the extraction sequence of Zr, Hf, and Rf from 8 M HCl into TBP, Günther et al. [80] have determined distribution coefficients of these elements from HCl solutions. In 8 M HCl, the K_d of Zr is 1180, that for Hf is 64. This difference makes possible a chromatographic separation of Hf from Zr in ARCA II on 1.6×8 mm columns filled with TBP on an inert support. This separation was also studied with the short-lived ^{169}Hf from the $\text{Gd}(^{18}\text{O}, \text{xn})$ reaction yielding $K_d = 53_{-13}^{+15}$ in agreement with the above results from batch extraction experiments. 78-s ^{261}Rf was produced in the $^{248}\text{Cm}(^{18}\text{O}, 5\text{n})$ reaction and from the distribution of α -events between the Hf- and Zr-fraction, a K_d value of Rf in 8 M HCl of 150_{-46}^{+64} was determined. This gives the extraction sequence $\text{Zr} > \text{Rf} > \text{Hf}$. Such a sequence is expected from theoretical considerations [80,110] of complex formation and the concurrent hydrolysis of complexes



To predict the equilibrium constant of eq. 11, one has to consider the difference in total energies of the (partially) hydrolyzed species on the left-hand side of eq. 11 that are not extracted and the extractable MCl_4 . (It is assumed that the OH^- containing species will not extract into the organic phase because of the strong hydrogen bonding interaction between OH^- and H_2O .) This can be done by quantum chemical calculations, presently using DS DVM [7,8], allowing the separate determination of the differences in the Coulomb and the covalent parts of the binding energy. Calculations for Zr, Hf, and Rf are still to be done, but one can already draw qualitative conclusions based on a parallel study of the hydrolysis of chloro complexes of the group 5 elements Nb, Ta, Pa, and Db [110]. For group 5, the order of complex formation described by equilibria similar to the reaction (eq. 11) in 4–12 M HCl solutions was theoretically predicted to be $\text{Pa} > \text{Nb} > \text{Db} > \text{Ta}$ in excellent agreement with experimental data [81] to be discussed in Section 6. The reason for this is the dominant difference in the Coulomb part of the energy of reaction when OH^- groups are replaced by Cl^- anions. Earlier calculations [100] for MCl_4 ($\text{M} = \text{Zr}, \text{Hf}, \text{and Rf}$) have shown that the compounds are very similar, which can also be supposed for $\text{M}(\text{OH})_x\text{Cl}_{4-x}$. Knowing the analogy in the electronic structure of the halides and oxohalides of groups 4 and 5 [8,110], one can postulate the same order of complex formation $\text{Zr} > \text{Rf} > \text{Hf}$ according to eq. 11 as was found for the corresponding group 5 elements. For both groups 4 and 5, such a sequence is in full agreement with experimental data for Zr, Hf, and Nb, Ta, respectively, showing that compounds of the 5d elements are more hydrolyzed than those of the 4d elements and are hence less extracted. For these elements, the hydrolysis of complexes [7,110] is in opposite order to the hydrolysis of cations. This indicates that the conclusions in [75,76], that the seemingly low extraction of Hf and Rf is due to their increased tendency to hydrolyze, are incorrect.

Fluoride complexation of the group 4 elements was studied by Szegłowski et al. [85,86], by Pfrepper et al. [87,88], and by Strub et al. [83]. In [86], ^{261}Rf transported to the chemistry apparatus online, was continuously dissolved in 0.2 M HF, and the solution was passed through three ion-exchange columns. In the first cation-exchange column, the transplutonium elements produced directly in the $^{18}\text{O}+^{248}\text{Cm}$ reaction were removed from the solution. In the next anion-exchange column, ^{261}Rf was sorbed as RfF_6^{2-} , while the following cation-exchange column retained its cationic decay products. After the end of bombardment, the descendents ^{253}Fm and ^{253}Es were desorbed from the third column and detected offline by α -spectroscopy. Their detection was proof that Rf forms anionic fluoride complexes, which are sorbed on an anion-exchange resin.

By selecting conditions such that the retention time t_r is of the order of the nuclear half-life, $t_{1/2}$, Pfrepper et al. [87,88] determined $K_d = 13.9 \pm 1.1$ ml/g for short-lived Hf isotopes in 0.2 M $\text{HNO}_3/0.27$ M HF by online chromatography using the three-column technique. By varying the HNO_3 molarity to 0.5 M—the nitrate is hereby used as a counterion— K_d was lowered to 2.4 ± 0.8 ml/g. For the plot of $\log K_d$ vs. $\log [\text{NO}_3^-]$ [87], the slope of -1.9 ± 0.4 is a measure of the ionic charge of the fluoride complex; it is in good agreement with the slope of -2.0 found in batch experiments. The structure of the extracted complex is thus HfF_6^{2-} . In experiments with ^{261}Rf [88], in which Hf isotopes were simultaneously produced (due to an admixture of nat. Gd in the ^{248}Cm target) K_d values for Hf and Rf were simultaneously determined and an ionic charge of -2 was also ascertained for Rf (0.1 M $\text{HNO}_3/0.27$ M HF and 0.2 M $\text{HNO}_3/0.27$ M HF).

The K_d values for Hf and Rf are indistinguishable at both counterion concentrations. Thus, the gain of information about specific chemical properties of Rf in comparison to those of Zr and Hf in [88] is rather limited. It is tempting to comment on this with the following general statement. In order to learn about specific differences in the chemical properties of the transactinides, with respect to the properties of their lighter homologs and pseudohomologs, one should not select conditions (e.g., ligand concentrations) under which the properties show *saturation*. Rather, it is much more informative to select conditions where the properties of the homologs experience a *threshold*. Examples for such threshold behavior are (i) the yield-vs.-temperature curves in isothermal gas chromatography where the threshold behavior (and the related adsorption enthalpy) characterizes a given element, or (ii) the threshold for chloride complex formation of Zr, Hf, and Rf in 8 M HCl [80] and extraction into TBP where the distinct extraction sequence $\text{Zr} > \text{Rf} > \text{Hf}$ can be reproduced as a consequence of competing chloride complexation and metal ion hydrolysis.

Testing the threshold behavior in the fluoride complexation of the group 4 elements is the theme of the ongoing work of Strub et al. [83] utilizing ARCA II and the chemical system used in the first study of the aqueous chemistry of Sg [82], i.e., 0.1 M HNO_3/x M HF (x variable). For Mo, W, and Sg, 0.1 M $\text{HNO}_3/5 \times 10^{-4}$ M HF was found to be efficient and selective in eluting these elements from 1.6×8 mm cation-exchange columns filled with Aminex A6 [82]. At this molarity of HF, Zr and Hf were known to be strongly retained on the column as cations with K_d values $\sim 10^3$. ^{261}Rf and ^{169}Hf produced by the ^{18}O bombardment of a mixed $^{248}\text{Cm}/\text{Gd}$ target show the same behavior. For Zr and Hf, the fall of the K_d values owing to the formation of fluoride complexes occurs between 10^{-3} M HF and 10^{-2} M HF. For Rf, the K_d value in 0.1 M $\text{HNO}_3/10^{-2}$ M HF is still high (>312), and complete elution is only achieved in 0.1 M $\text{HNO}_3/0.1$ M HF [83]. This threshold behavior is between that of Zr, Hf, and that of Th.

It is remarkable that the K_d values for Zr and Hf on an anion-exchange resin *rise* in the same HF concentration range (0.1 M $\text{HNO}_3/10^{-3}$ M HF through 10^{-2} M HF) in which they *fall* on the cation exchanger. This indicates that the formation of anionic fluoride complexes takes place simultaneously with the disappearance of the cationic species. Conversely, the Rf data on the anion-exchange resin [83] do not rise in 0.1 M $\text{HNO}_3/(10^{-2}$ through 0.5 M HF) again resembling the behavior of Th. It is difficult to reconcile this with the data given by Pfrepper et al. [88] for 0.1 M $\text{HNO}_3/0.27$ M HF on the special anion exchanger Wofafit HS 36 where both Hf and Rf have K_d values of the order of 50. Further, the K_d values by Strub et al. [83] on a standard anion exchanger in 0.1 M $\text{HNO}_3/(>10^{-2}$ M HF) are ~ 8 for Rf and ~ 200 for Zr and Hf. Standard anion exchangers contain $-\text{N}^+(\text{CH}_3)_3$ as functional group, whereas Wofafit HS36 contains $-\text{N}^+(\text{C}_2\text{H}_5)_3$ groups that show a higher selectivity for the counter ion NO_3^- . Whether the different functionalizations and selectivities can account for the different results in [88] and [83] must be further investigated.

5.3 Evaluation

While earlier MCDF calculations [95] had predicted a $[\text{Rn}]5f^{14}6d7s^27p_{1/2}$ electron configuration for Rf, more recent CCSD calculations predict $[\text{Rn}]5f^{14}6d^27s^2$ as the ground-state configuration [97] mak-

ing Rf a typical group 4 element, which should have no similarity to the p-element Pb. This was confirmed experimentally [106].

The volatility of the group 4 tetrachlorides in quartz-glass columns in [103] shows the sequence $Zr \geq Rf > Hf$. In view of the large uncertainties, this may not yet be considered as firmly established. In the presence of oxygen, "reaction gas chromatography" is performed with the less volatile oxochlorides [63]. For Rf, the characteristic temperature, $T_{50\%}$, is shifted from 125 °C for the tetrachloride to 325 °C for the oxochloride.

For the bromide compound $RfBr_4$, the yield-vs.-temperature curve is shifted by about 150 °C to higher temperatures compared to the $RfCl_4$ curve. Also in the case of bromides, Hf shows a lower volatility than Rf.

In the aqueous phase, strong complexing of Rf^{4+} by α -HIB [13] and by Cl^- [14] was demonstrated.

Liquid-liquid extractions of the neutral chlorides into TBP/benzene [73,75] were severely hampered by losses of Hf and Rf by sorption on Teflon surfaces. These experiments and their inappropriate interpretation [75] were criticized [80], and the sequence of extraction into TBP, $Zr > Rf > Hf$, was firmly established [80]. The latter is in agreement with theoretical considerations taking into account the competition between chloride complex formation and hydrolysis of the chloride complexes [80].

The hydrolysis of the metal ions Zr^{4+} , Hf^{4+} , and Rf^{4+} in dilute HCl solutions [74] needs to be re-examined, as the published data for Rf^{4+} are in contradiction to expectations based on the electrostatic model of the hydrolysis mechanism.

In HF solutions, the formation of anionic fluoride complexes of Rf was established in [86]. In 0.27 M HF with various concentrations of the counter ion NO_3^- [88], it was established that RfF_6^{2-} is the complex undergoing anion-exchange with a K_d value indistinguishable from those for Zr and Hf. This is in disagreement with [83] where large differences of the K_d values for Rf on the one hand and Zr and Hf on the other hand in mixed HNO_3 /HF solutions were measured both on cation- and anion-exchange resins. This makes a re-examination of the data in [88] desirable.

Theoretical calculations for the fluoride complexes of Zr, Hf, Th, and Rf are needed in order to understand the large differences in the ion-exchange behavior between Rf and its lighter homologs Zr and Hf [83].

6. DUBNIUM (ELEMENT 105)

6.1 Theoretical predictions

In the periodic table, Db is placed in group 5 below Ta, so that the electronic ground-state configuration is expected to be $[Rn]5f^{14}6d^37s^2$. This is in agreement with early relativistic calculations [92] and with a recent MCDF calculation [111]. Thus, a significant contribution of the $7p_{1/2}$ state to the ground state is not expected for Db. Atomic and ionic radii and the first through fifth ionization potentials were calculated in [111]. Differences between the chemical behavior of Db and the extrapolated properties of an eka-tantalum could result from a larger ionic radius, a different effective charge, and a different radial extension of the 6d orbitals, which are most important in its molecular bondings [100,110–115]. Redox potentials were estimated for the group 5 elements, including the pseudohomolog Pa, on the basis of ionization potentials from MCDF calculations [111,116]. It was shown that the stability of the pentavalent state increases from V to Db, while the stability of the tetra- and trivalent state decreases. Although it was found that the stability of the maximum oxidation state decreases in going from Lr to Db, no extra stability of the trivalent state in Db was found [116]. It would be interesting to test this prediction in reduction experiments similar to the experiments performed on Lr [117].

DS DVM calculations allow prediction of the degree of covalency in the bonding and the effective charge on the central atom in halide and oxohalide compounds of the group 5 elements [112–115].

From these, it was inferred [113] that DbBr_5 should be more volatile than its lighter homologs, whereas classical extrapolations within the periodic table would yield a lower volatility [20].

The electronic structures of the group 5 anionic complexes $[\text{MCl}_6]^-$, $[\text{MOCl}_4]^-$, $[\text{M}(\text{OH})_2\text{Cl}_4]^-$, and $[\text{MOCl}_5]^{2-}$ were calculated with the DS DVM code [118]. By applying Born's theory of phase transition between the aqueous phase and the organic phase (mixed HCl/HF solutions and TiOA [77]) the extraction sequence $\text{Pa} > \text{Db} > \text{Nb}$ was predicted, which is the inverse of that observed experimentally [77]. Due to the complicated situation in mixed HCl/HF solutions, with possibilities for forming mixed chloride/fluoride or fluoride complexes, it was recommended that the experiments in the pure HCl system should be repeated [118]. While these new experiments were prepared [123], V. Pershina [110] considered hydrolysis and complex formation of Nb, Ta, Pb, and Pa in HCl solutions as competing processes in equilibria such as



Here, the hydrolyzed species on the left is the one staying in the aqueous phase, and the chloride complex on the right is expected to be extracted into the amine phase. Calculations of the electronic structures of the hydrolyzed species of Nb, Ta, Db, and Pa, and of their complexes in HCl solutions, were performed [110] using the DS DVM method. On the basis of results of these calculations, relative values of the free energy change for the complex formation reactions were determined [110]. The order of complex formation above 4 M HCl was found to be $\text{Pa} \gg \text{Nb} > \text{Db} > \text{Ta}$. This sequence is predominantly defined by the electrostatic energy of the metal–ligand interaction. The hydrolysis of the chloride complexes, as a reverse process, was found to change as $\text{Ta} > \text{Db} > \text{Nb} \gg \text{Pa}$. Finally, using Born's theory of metal-ion extraction, the following trend in the extraction of the anionic species from aqueous solutions containing >4 M HCl was predicted [110]: $\text{Pa} \gg \text{Nb} \geq \text{Db} > \text{Ta}$. This was the first time that detailed predictions of the aqueous-phase properties of these elements were made. It shows that a detailed analysis of the electronic structure of the compounds formed under specific conditions is necessary and leads to the prediction of an *inversion of the trend of the properties when going from the 5d to the 6d elements*. This has already been observed for the group 4 elements [80], and it is of importance to verify this experimentally for the group 5 elements.

6.2 Experimental results

The volatilities of the chlorides and bromides of Db were first studied with 1.8-s ^{261}Db in a thermochromatographic apparatus similar to that used for Rf [15,16]. In the volatility study of the bromides, the SF track distribution detected on mica track detectors along the chromatographic column was assumed to characterize the behavior of Db. The measured distribution of ^{261}Db was corrected for its much shorter half-life before comparing it with the adsorption zones of longer-lived tracer activities of various elements, including 3.3-min ^{169}Hf and 14.6-h ^{90}Nb . The corrected data characterize Db bromide as being less volatile than Nb bromide and close in volatility to Hf bromide.

The first isothermal gas chromatography experiments with the bromides of the group 5 elements Nb, Ta, and Db [58,66] were performed with an earlier version of the OLGA apparatus. The yields for Nb were measured with HBr as brominating agent, for Ta, HBr plus BBr_3 vapor was used, and for Db, both HBr and HBr plus BBr_3 vapor were applied. Within the error limits, the bromides of Nb and Ta have the same volatility, while the Db bromide is less volatile, as already indicated by the thermochromatographic data [16]. Both sets of experimental data seem, at first glance, to disagree with results from relativistic molecular calculations [113]. Theory predicts that DbBr_5 has the highest covalency and lowest effective charge among the group 5 bromides, which should make DbBr_5 more volatile than its homologs. Also, a “nonrelativistic” thermodynamical model [119] leads to the prediction of a band of DbBr_5 volatilities that are close to those of NbBr_5 and TaBr_5 .

The current interpretation of the low Db-bromide volatility is the possible formation, owing to the presence of traces of oxygen in the system, of the oxotribromide DbOBr_3 instead of the pentabromide. This is supported by theoretical calculations, which show a much stronger tendency for Db to form oxohalide compounds than for Nb and Ta [114]. While the generally lower volatility of the oxohalide can be inferred from the DS DVM calculations, it remains open whether the DbOBr_3 volatility will be higher or lower than that of the Nb and Ta oxohalides [114]. It is also conceivable that the lower volatility of the oxobromides is associated with reaction gas chromatography. Further investigations are needed to clarify the situation.

In a series of experiments investigating the volatility of the chlorides of the group 5 elements, it was observed that the Db chlorides are more volatile than the bromides, and possibly similar in volatility to NbCl_5 [20,120]. This is in agreement with the finding that the groups 4 and 5 chlorides are more volatile than the respective bromides. For Ta, only a species with a much lower volatility was observed, presumably TaOCl_3 [20].

In the most recent experiment [67], either precautions were taken to keep the partial pressure of oxygen as low as possible, or controlled partial pressures of free O_2 were applied to study the volatility of the chlorides of Nb and Db.

This experiment reveals that the concentration of O_2 and oxygen-containing compounds (e.g., H_2O) is critical in volatility experiments with group 5 elements and needs to be controlled carefully. For a volume fraction of oxygen below 1 ppm, NbCl_5 is formed with purified HCl as chlorinating agent. For a volume fraction of oxygen between 1 ppm and 80 ppm, two species of different volatilities (NbCl_5 and NbOCl_3) are observed. Both species were produced in about equal amounts, which resulted in a yield curve with two steps. Finally, above a volume fraction of oxygen ≥ 80 ppm, NbOCl_3 was identified as the volatile species. The conditions at which the subsequent experiments with ^{262}Db were conducted were as close as possible to the conditions where NbCl_5 was formed in the test experiments. The relative yield curve for ^{262}Db consists of two steps suggesting that both DbCl_5 and DbOCl_3 were present [67]. $\Delta_{\text{ads}}H^\circ(\text{DbOCl}_3) = -117 \text{ kJ mol}^{-1}$ was obtained in the application of the Monte Carlo model at the higher temperatures, and only a lower limit of $\Delta_{\text{ads}}H^\circ(\text{DbCl}_5) > -98 \text{ kJ mol}^{-1}$ can be given for the pentachloride. An investigation of the Ta volatility is needed to complete the picture. Also, future experiments should extend the yield measurements of Db chlorides to lower temperatures for a comparison with theoretical predictions. At this time, the data show that, indeed, Db has a strong tendency to form the oxochloride as predicted.

First studies of the aqueous phase chemistry of Db were conducted by Gregorich et al. [50]. Like Nb and Ta, Db was adsorbed on glass surfaces upon fuming with nitric acid. In 801 manually performed experiments, 24 α -events due to the decay of 34-s ^{262}Db or its 3.9-s ^{258}Lr daughter, including 5 $\alpha\alpha$ -mother-daughter correlations were observed. In an attempt to study the extraction of the Db fluoride complex from 3.8 M HNO_3 /1.1 M HF into methyl isobutyl ketone (MIBK), no decays attributable to ^{262}Db could be observed. Under these conditions, Ta extracts, while Nb does not. From an extrapolation in group 5, it was expected that Db would behave more like Ta than Nb but, surprisingly, Db apparently did not extract. The non-Ta-like behavior of Db might indicate that Db forms polynegative anions like $[\text{DbF}_7]^{2-}$ under the chosen conditions. The higher charge would then prevent extraction even into solvents with a relatively high dielectric constant such as MIBK.

To investigate this unexpected finding and more facets of Db chemistry, a large number of automated separations were conducted with ARCA II [84]. In the first experiments, extraction chromatography separations with the liquid anion exchanger TiOA on an inert support [77] were performed. TiOA extracts all group 5 elements including Pa from HCl solutions above 10 M, irrespective of the formation of mono- or polynegative anions. At lower concentrations, selective back extractions were conducted to distinguish between the chemical behavior of Nb, Ta, Pa, and Db. Small amounts of HF (typically 0.02 M) were added to the HCl solutions, as this is recommended in the literature [121] to prevent hydrolysis and “to maintain reproducible solution chemistry” of the group 5 elements. Db was shown [77] to extract from 12 M HCl/0.02 M HF into the TiOA on the chromatographic columns in ARCA II,

as do Nb, Ta, and Pa, owing to the formation of anionic halide complexes. In subsequent elutions, the elution positions of Db relative to those of Nb, Ta, and Pa were determined [77] in 10 M HCl/0.025 M HF, in 4 M HCl/0.02 M HF, and in 0.5 M HCl/0.01 M HF [79]. 2198 collection and separation cycles on a 1-min time scale [77,79] were conducted to obtain K_d values for these three mixed HCl/HF solutions.

It was found that Db shows a striking non-Ta-like behavior and that it follows, at all HCl concentrations below 12 M, the behavior of its lighter homolog Nb and that of its pseudohomolog Pa. From this similarity, it was concluded that the complex stoichiometry for Db was $[\text{DbOX}_4]^-$ or $[\text{Db}(\text{OH})_2\text{X}_4]^-$. The preferential formation of oxohalide complexes of Db was also predicted theoretically [118]. As discussed in Section 6.1, owing to the complicated situation in mixed HCl/HF solutions, it was recommended [118] to repeat the experiments in the pure HCl system.

The similarity of the Db and Pa behavior in the TiOA experiments was the reason for performing a series of extractions of Db into diisobutyl carbinol (DIBC), a secondary alcohol that is a specific extractant for Pa. The extraction from concentrated HBr in ARCA II was followed by the elution of a Nb fraction in 6 M HCl/0.0002 M HF, and a Pa fraction in 0.5 M HCl. The number of ^{262}Db decays observed in the Nb fraction indicated that less than 45 % of the Db was extracted into DIBC and the extraction sequence $\text{Db} < \text{Nb} < \text{Pa}$ was established [78]. This was tentatively attributed to an increasing tendency of these elements to form nonextractable polynegative complex species in the sequence $\text{Pa} < \text{Nb} < \text{Db}$.

Another series of experiments with Db used its complexation by the α -HIB anion, $(\text{CH}_3)_2\text{COH-COO}^-$, which depends strongly on the charge of the metal ion [41]. Elutions from cation-exchange columns in ARCA II with unbuffered 0.05 M α -HIB showed that Db, together with Nb, Ta, and Pa, elutes promptly (within 4 s) while tri- and tetravalent ions are strongly retained on the resin [41]. This provided an unambiguous proof that pentavalent Db is the most stable valence state in aqueous solution. These separations, being fast and very clean, were also used to detect the hitherto undiscovered isotope 27-s ^{263}Db produced in the $^{249}\text{Bk}(^{18}\text{O}, 4n)$ reaction [40,41].

As suggested in [118], the amine extractions of the group 5 elements were systematically revisited by W. Paulus et al. [81,123]. V. Pershina [110], by considering the competition between hydrolysis and halide complex formation, predicted the extraction sequence $\text{Pa} \gg \text{Nb} \geq \text{Db} > \text{Ta}$, as mentioned above. K_d values for Nb, Ta, and Pa were measured in new batch extraction experiments with the quaternary ammonium salt Aliquat 336 and pure HF, HCl, and HBr solutions [81,123]. Based on these results, new chromatographic column separations with ARCA II were initiated to study separately the fluoride and chloride complexation of Db. As an example, the separation of Eu, Ta, Nb, and Pa tracers in the Aliquat 336/HCl system is as follows. The activities were fed onto the column in 10 M HCl. Trivalent actinides modeled by trivalent Eu would run through the column. Ta is eluted in 6 M HCl, Nb in 4 M HCl, and Pa in 0.5 M HCl [81,123].

The experiments with Db were conducted with a cycle time of 50 s. In the system Aliquat 336/HCl, after feeding the activity onto the column in 10 M HCl, a Ta fraction was eluted in 6 M HCl. This was followed by stripping of a combined Nb, Pa fraction from the column in 6 M $\text{HNO}_3/0.015$ M HF. From the distribution of α -decays between the Ta fraction and the Nb, Pa fraction, a K_d value of 438^{+532}_{-166} for Db in 6 M HCl was deduced which is close to that for Nb and differs from the values for Pa and Ta. Thus, the extraction sequence is $\text{Pa} > \text{Nb} \geq \text{Db} > \text{Ta}$, exactly as theoretically predicted [110].

In the system Aliquat 336/HF, the reaction products were loaded onto the column in 0.5 M HF. In elutions with 4 M HF (Pa fraction), and with 6 M $\text{HNO}_3/0.015$ M HF (combined Nb, Ta fraction) all α -decay events of Db were observed in the Nb, Ta fraction. This results in a lower limit for the K_d value of Db in 4 M HF of >570 , which is close to that for Nb and Ta ($\geq 10^3$) and differs markedly from that for Pa (~ 10).

It is satisfying to see that not only the extraction sequence in the system Aliquat 336/HCl is correctly predicted by theory [110] but that the calculated free-energy changes for the complex formation

reactions are of the order of 12 eV for the fluorides, 20 eV for the chlorides, and 22 eV for the bromides [122] (not taking into account the free energy of formation of H_2O , which is 3 eV), which is in agreement with the experimental findings. For the fluorides, the equilibrium is always on the right-hand side of eq. 12 even at low HF concentrations [123]; for the chlorides, it takes >3 M HCl to form extractable chloride complexes, and for the bromides, the threshold is shifted to >6 M HBr [123].

To conclude, the amine extraction behavior of Db halide complexes is always close to that of its lighter homolog Nb, in agreement with the predicted *inversion of the trend of the properties when going from the 5d to the 6d elements* [110,122]. In pure HF solutions, it differs most from the behavior of Pa. In pure HCl solutions, it differs considerably from both Pa and Ta. In mixed HCl/HF solutions, it differs markedly from the behavior of Ta. The studies of the halide complexing and amine extraction of the group 5 elements both theoretically [110,122] and experimentally [81,123] demonstrate that enormous progress has been made in understanding detailed facets of the chemistry of the transactinide elements.

6.3 Evaluation

With the electronic ground-state configuration $[\text{Rn}]5f^{14}6d^37s^2$, Db is a member of the group 5 elements. DS-DVM calculations [112–115] suggest that the pentahalides of Db should be more volatile than those of its lighter homologs. Experimental volatility studies have failed to demonstrate this. For the group 5 bromides [58,66], the lower volatility of the Db species is discussed in terms of the formation of the oxotribromide DbOBr_3 .

In [67], it was explicitly shown for the chlorides of Nb and Db that the concentration of O_2 and oxygen-containing compounds is extremely critical in volatility experiments with the group 5 elements and that $T_{50\%}$ is shifted from 150 °C for NbCl_5 to 250 °C for NbOCl_3 . Indications for the presence of two components in the yield-vs.-temperature curve for Db were also observed in [67], suggesting the existence of both DbCl_5 and DbOCl_3 . However, the adsorption enthalpy for DbCl_5 (i.e., its volatility relative to those of Nb and Ta) still needs to be determined.

In aqueous solutions, sorption of Db on glass surfaces [50] and its strong complexing by α -HIB [41] are well established. The halide complex formation was studied by extraction chromatography with aliphatic amines [77,81]. In 6 M HCl/Aluquat 336, the extraction sequence $\text{Pa} > \text{Nb} \geq \text{Db} > \text{Ta}$ is observed, exactly as theoretically predicted [110] by explicitly considering the competition between the chloride complex formation and hydrolysis reactions. This leads to the prediction of an inversion in the trend of properties when going from the 5d to the 6d elements [110]. Also, the sequence of extraction into the amine

fluorides \gg chlorides $>$ bromides

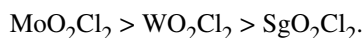
is correctly predicted by theory.

7. SEABORGIUM (ELEMENT 106)

7.1 Theoretical predictions

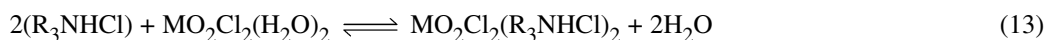
Relativistic MO calculations [100,124] with the DS DVM code have shown that the volatile species SgCl_6 as well as SgOCl_4 will decompose at high temperatures, analogous to MoCl_6 and MoOCl_4 , which decompose into compounds of Mo(V). Therefore, DS DVM calculations were performed on the electronic structure of the group 6 dioxodichlorides MO_2Cl_2 ($\text{M} = \text{Cr}, \text{Mo}, \text{W}, \text{Sg}$) and an analysis with respect to the stability of their compounds toward thermal decomposition. In the framework of the Mulliken analysis [125,126], effective charges Q_M , overlap populations, OP, and dipole moments, μ , were determined.

The trends in Q_M , OP, and the metal–ligand bond energies are reminiscent of those for the group 6 oxotetrachlorides, $MOCl_4$. However, the energy gaps ΔE between the highest occupied molecular orbital (HOMO) and the lowest unoccupied molecular orbital (LUMO) are much larger for the dioxodichlorides, MO_2Cl_2 , than for the oxotetrachlorides. This should prevent the dioxodichlorides from thermal dissociation and should make MoO_2Cl_2 , WO_2Cl_2 , and SgO_2Cl_2 much more stable than $MoOCl_4$, $WOCl_4$, and $SgOCl_4$ even though their M–Cl bond strengths are similar. The lower volatility of WO_2Cl_2 compared to that of MoO_2Cl_2 was associated [125,126] with the larger dipole moment of the former compound. And from the trend in dipole moments, the following sequence for the order of decreasing volatility was predicted:

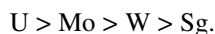


These theoretical results [100,124–126] corroborate the decision of the gas-phase chemists to use oxygen-containing chlorinating agents, and the volatility data (Section 7.2) are consistent with predictions. We note in passing that the dipole moments in the dioxodichlorides of the group 6 elements are the result of the ds hybridization in MO_2^{2+} giving rise to a *cis* configuration of the oxygen ligands [125].

DS DVM calculations [100,124,125] confirmed the full analogy between SgO_2Cl_2 and MO_2Cl_2 ($M = Mo$ and W). Thus, one can also assume the same type of complexes of Sg in HCl and HF solutions as those of Mo and W. Results for the extraction of the Mo, W, and U species from aqueous HCl solutions into organic media have shown the opposite trend in the distribution coefficients, $K_d(U) > K_d(Mo) > K_d(W)$, than for HF solutions where $K_d(U) < K_d(Mo) < K_d(W)$. Pershina associates this with two different extraction mechanisms [8]. In the HCl case, the mechanism of formation of an adduct is valid:

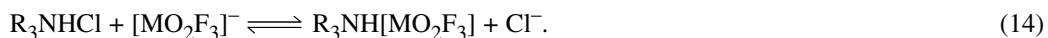


The process of molecule transfer (ΔG_t) between the aqueous and the organic phase in this case is defined by the strength of the dipole–dipole interaction of the $MO_2Cl_2(H_2O)_2$ species with water molecules. The values of dipole moments obtained as a result of the DS DVM calculations [125], indicate the distribution coefficients in 2–6 M HCl should be in the sequence



The absence of a dipole moment in $UO_2Cl_2(H_2O)_2$ with a linear structure of the oxygen ligands, explains its superior extractability.

In HF solutions, anion-exchange takes place [8] according to



Here, the free energy of transfer is determined by the sizes of the extracted species, leading to the sequence



The distribution coefficient is finally dependent on the complex formation and on the partition of the complexes between the phases. Details of the electronic structure of the anionic complexes existing in HF solutions still need to be studied.

Based on DS DVM calculations of $[MO_4]^{2-}$ [128], a linear correlation between calculated energies of the charge-transfer transitions related to the reduction process $M^{6+} \rightarrow M^{5+}$ and the reduction potentials $E^\circ(MO_4^{2-}/MO_4^{3-})$ was used to estimate $E^\circ(SgO_4^{2-}/SgO_4^{3-})$ as -1.60 V. An increased bond length of 0.03 \AA would yield a value of -1.34 V. For the transactinide series, the stability of the highest oxidation state decreases as



Thus, it might be interesting to attempt to reduce Sg by contact with a strongly reducing metal such as Al ($E^\circ = -1.662$ V) in future experiments.

7.2 Experimental results

First attempts to chemically characterize Sg were reported by Timokhin et al. [55] in 1992 and were completed in 1993 and 1995 [56,57]. The authors used the short-lived isotope 0.9-s ^{263}Sg produced in the $^{249}\text{Cf}(^{18}\text{O},4n)$ reaction and their fast online thermochromatography equipment. The recoils were thermalized and swept from the target chamber in 1 l/min argon gas directly into the thermochromatographic column—an open, 3.5-mm i.d. tube of fused silica, 120 cm in length. About 60 % of the recoils reached the column; the rest deposited on the walls of the target chamber. At the column inlet, the flowing argon was mixed with the reactive gas supplied from the end part of the apparatus through an annular channel formed by the glass jacket of the column. At 0.2 l/min, air saturated with SOCl_2 vapor was supplied to yield partial pressures of 20-mm Hg (or 2.6 vol %) of SOCl_2 and 25-mm Hg (or 3.3 vol %) of O_2 in the resulting carrier gas.

In test experiments with Mo and W radioisotopes with half-lives in the range of seconds to hours, Yakushev et al. [56] generally observed two deposition zones, a “high temperature zone” at about 250 °C and a “low temperature zone” at about 160 °C. The distribution of the activities between these zones depended on the half-life, such that the percentage deposited in the lower temperature zone increased with increasing half-lives of the nuclides. This was interpreted as evidence for a rapid formation of the dioxodichlorides, MO_2Cl_2 , that are subsequently relatively slowly converted into the more volatile oxotetrachlorides, MOCl_4 . For very short-lived species, a deposition on the quartz surface as the dioxodichloride was expected. Zvara et al. [57] also report that, in their thermochromatography column, short-lived W isotopes reached their deposition zone in less than 0.8 s.

In the Sg experiments by Zvara et al. [57], the inner surface of the fused silica column served as a solid-state detector for SF events. After the discovery of the α -emitting 0.9 ± 0.2 -s ^{263}Sg by Ghiorso et al. [129] with a cross-section on the order of 0.3 nb, Druin et al. [130], had reported observation of a $0.64^{+0.32}_{-0.18}$ s SF activity, which they assigned to ^{263}Sg with 0.6 nb cross-section at 95 MeV. This was thought to be the origin of the fission tracks in the fused silica column of Zvara et al. [57], which were made visible by etching with HF subsequent 5-cm segments of the column and scanning the surface with an optical microscope. At room temperature, the detection efficiency with this technique is 65 %. It decreases at higher temperatures due to annealing of the tracks.

Six experiments with the $^{249}\text{Cf}(^{18}\text{O},5n)^{263}\text{Sg}$ reaction were performed by Zvara et al. [57] with integral doses of ^{18}O ions between 0.8 and 2.6×10^{17} ions each. In the first two thermochromatographic runs, a quartz wool filter was present in the start zone as in most ancillary tests. No fission tracks were found in the column. In the four following experiments, this filter was omitted. In the fifth experiment, no chlorinating reagents were added, and the column was kept at ambient temperature to test the behavior of the nonvolatile actinides. Eighteen SF events were detected within the first 15 cm of the column. The number of tracks found in runs 3, 4, and 6 are 10, 20, and 11, respectively, and these are mostly distributed between a distance along the column of 20–120 cm.

After corrections for the decreased detection efficiency in the hotter part of the column, the distribution of fission tracks is compared with the distribution of gamma activity due to 2.5-h ^{176}W . One notices a marked difference in the deposition temperatures of Sg and ^{176}W . According to [57], this difference can hardly be associated with the different half-lives, 0.9 s vs. 2.5 h, resulting in different migration times [18]. Rather, according to [57], the different deposition zones for ^{263}Sg and ^{176}W point to nonidentical chemical states of the two homologs: the short-lived ^{263}Sg deposited as SgO_2Cl_2 and decayed long before this compound could be transformed into SgOCl_4 . The long-lived ^{176}W first rather quickly formed WO_2Cl_2 , but subsequently was completely converted into the more volatile WOCl_4 . In the first two “unsuccessful” experiments, the retention time of Sg on the quartz wool filter was assumed [57] to have exceeded the nuclear half-life of the Sg isotope(s). A longer retention time on the filters

than in the open column was observed earlier by the authors in investigations of the groups 4 and 5 elements and was attributed to the large effective surface of the quartz filters (equivalent to several meters of an open column).

The work by the Dubna group [55–57] has been met with skepticism [143]. This concerns both the assignment of the observed SF activity and the chemical selectivity of the chemical separation for Sg.

The first concern is with the assignment of the observed SF activity. The 70 % SF branch deduced on the basis of cross-section arguments by Druin et al. [130] has never been confirmed. In the decay chains of $^{271}110$ as third-generation α -decays, 8 α -decays of ^{263}Sg grouped around 9.248 MeV were measured [131] in excellent agreement with the 9.25 MeV literature value [129] for 0.9-s ^{263}Sg , but the half-life of $0.31^{+0.16}_{-0.08}$ s is different. Therefore, and because in [131] the 9.06 MeV line was not observed (intensity ratio 9.25 MeV:9.06 MeV in [129] is $\sim 9:1$), one must assign the two α -lines to two different levels in ^{263}Sg . Both are populated in the $^{249}\text{Cf}(^{18}\text{O},4n)$ reaction, but only the 0.3-s level is populated by α -decay in the decay chain of $^{271}110$. An upper limit for a fission or electron capture branch of the 0.3-s level of 12 % was given in [131]. Hofmann et al. [131] compared the decay pattern of ^{263}Sg with that of the next heavier $N = 157$ isotone ^{265}Hs . Two α -lines with energies of 10.31 and 10.58 MeV and an intensity ratio of 2:1 were measured in the case of the direct production in the reaction $^{58}\text{Fe}+^{208}\text{Pb}$. Only the 10.58 MeV transition was observed in the α -decays of $^{269}110$ [132]. Therefore, two levels with approximately the same half-life of 1.5 ms exist in ^{265}Hs . As fission was not observed, one can determine the α -decay hindrance factors as 1.1 (10.31 MeV) and 5.0 (10.58 MeV) both being in agreement with favored α -transitions. This also confirms the expectation, based on theoretical predictions [133], of the existence of isomeric states with similar decay properties. Theory predicts a very similar level structure for the lighter odd-A isotones. If this is the case in ^{263}Sg , the 0.9-s state should also decay by favored α -transition. Also, a fission branch of more than 10 % in ^{263}Sg would require an odd-N fission hindrance factor of less than 200 (usually on the order of 10^5 for odd neutrons). These arguments [131] do not rule out a large fission branch in ^{263m}Sg , but let it appear unlikely.

Thus, if the assignment of the observed SF events in the thermochromatography experiments [57] to the decay of 0.9-s ^{263m}Sg is questionable, it is of crucial importance to show that in the experiments the other transactinide elements Rf and Db are much less volatile than the studied Sg compound. Zvara et al. [57] do claim that Rf and Db do not form volatile compounds with a chlorinating, oxygen-containing carrier gas, but the references given do not warrant such a claim. On the other hand, Türler et al. [67] have shown that DbOCl_3 is volatile above 200 °C, and an absorption enthalpy of -117 kJ/mol was deduced. From literature data, we know that DbOCl_3 is more volatile than TaOCl_3 . Therefore, DbOCl_3 could have been volatile under the experimental conditions of the experiment even if it had been shown that Ta was not volatile. A volatile DbOCl_3 needs to be considered because one cannot exclude an EC decay branch in ^{263m}Sg leading to SF in ^{263}Db [40] and, after α -decay, to SF in ^{259}Lr [134]. Such a “bizarre” explanation of the observed SF events in the Sg experiments [57] is not ruled out by the evidence presented.

Also for Rf, Jost et al. [63] showed that ^{261}Rf is volatile in a carrier gas of 1 l/min He, 150 ml/min Cl_2 saturated with SOCl_2 , and 20 ml/min O_2 , i.e., under conditions that are close to the conditions of the thermochromatography experiments [55–57].

In summary, the conclusion in [57] that only Sg can be responsible for the observed SF decays is not convincing. Even though the distribution of fission tracks in the thermochromatography column does not contradict the interpretation of the results as being due to Sg, the evidence presented in [57] falls short of demonstrating that other sources of SF tracks are rigorously excluded.

In 1991, an international collaboration centered around the nuclear chemistry groups at GSI, Darmstadt, the University of Mainz, and PSI, Villigen, started the chemical characterization of Sg in a series of test experiments, see, e.g., [135–138,127]. Generally, their experiments used gas-jet transportation systems and “external” detection systems in which the $\alpha\alpha$ -correlation technique with silicon detectors was used, both being “slow” compared to the Dubna technique [55–57]. Therefore, based on

the predicted enhanced nuclear stability near $N = 162$ and $Z = 108$ owing to an especially large negative shell correction [139], it was hoped that more neutron-rich nuclides with presumably longer half-lives than the 0.9 s of $^{263\text{m}}\text{Sg}$ could be synthesized, e.g., in the $^{22}\text{Ne} + ^{248}\text{Cm}$ reaction. Indeed, in 1993, working at the Dubna gas-filled recoil separator, a Dubna-Livermore collaboration succeeded to synthesize two new isotopes of Sg, ^{265}Sg and ^{266}Sg , in the $^{248}\text{Cm}(^{22}\text{Ne},5\text{n})$ - and $^{248}\text{Cm}(^{22}\text{Ne},4\text{n})$ -reaction at 121 MeV and 116 MeV, respectively [42]. They measured an α -energy of 8.63 ± 0.05 MeV for ^{266}Sg and a half-life of 1.2 s for the spontaneously fissioning daughter, ^{262}Rf . For ^{265}Sg , they measured α -energies between 8.71 and 8.91 MeV and correlated α -decays of the daughter ^{261}Rf (8.29 MeV) and the grand-daughter ^{257}No (8.222, 8.27, 8.32 MeV). The cross-sections were reported to be 80 pb at 116 MeV and 60 pb at 121 MeV for production of ^{266}Sg and 260 pb at 121 MeV for production of ^{265}Sg . These were reported to have an estimated uncertainty factor of ca. 3. Using the phenomenological formula of Viola and Seaborg in [139], they estimated a partial α -half-life for ^{266}Sg of 10 to 30 s and of 2 to 30 s for ^{265}Sg , assuming a hindrance factor between 1 and 3. Measurements of the life times could not be performed as the implantation signals in the position-sensitive surface barrier detector were below the detection threshold. The estimated half-lives were felt to be rather encouraging for the planned chemistry experiments with these Sg isotopes.

In 1995, two of the developed techniques [127,138] were eventually used to study the chemical properties of Sg. A short account of these successful first experiments and their results was published recently [43].

The choice of the chemical system was influenced by the wish to discriminate from the group 4 elements and by theoretical predictions [125], indicating that SgO_2Cl_2 should be the most stable oxochloride compound. Thus, chlorinating oxygen-containing reactive gases were selected. It was also predicted by calculating the dipole moments in the Mo-, W-, and Sg-dioxodichlorides [125] that the volatility should decrease in the order $\text{Mo} > \text{W} > \text{Sg}$. With the aid of an empirical correlation between sublimation enthalpy ($\Delta_{\text{sub}}H^\circ$) and adsorption enthalpy on quartz surfaces, $\Delta_{\text{ads}}H^\circ(\text{SgO}_2\text{Cl}_2) = -106$ kJ/mol was predicted [141].

With the reaction oven temperature kept at 900 °C and typically 100 ml/min Cl_2 saturated with SOCl_2 plus 2 ml/min O_2 , the chromatographic behavior of short-lived Mo nuclides from ^{235}U fission and of short-lived W isotopes in the $^{152}\text{Gd}(^{20}\text{Ne},x\text{n})$ reaction was studied. A $\Delta_{\text{ads}}H^\circ$ value of -90 kJ/mol was measured for MoO_2Cl_2 and of -100 kJ/mol for the less volatile compound WO_2Cl_2 . Also, the yield-vs.-temperature curve for ^{229}U from the $^{232}\text{Th}(\alpha,7\text{n})$ reaction was measured. It gave a $\Delta_{\text{ads}}H^\circ$ value of -91 kJ/mol indicative of the formation of UCl_6 [68]. It was demonstrated that for isothermal temperatures above 275 °C, retention times less than 10 s in OLGA III are achieved.

In a first experiment in 1995 at the GSI UNILAC accelerator, a ^{248}Cm target of $950 \mu\text{g}/\text{cm}^2$ was bombarded with 121 MeV ^{22}Ne ions of $3 \cdot 10^{12}$ ions \cdot s $^{-1}$. OLGA III was operated between 300 and 400 °C. As reactive agents, 100 ml/min Cl_2 saturated with SOCl_2 and 2 ml/min O_2 were added. SF decays and α -decays were registered in ROMA. The separated activities were deposited on thin polypropylene foils ($30\text{--}40 \mu\text{g}/\text{cm}^2$) at the periphery of a 64-position wheel. Every 10 s, the wheel was stepped to move the collected activity between 7 pairs of PIPS detectors. All events were registered in an event-by-event mode. Due to a long-lived contamination from ^{212}Po in the 8.8 MeV region, where α -decays of ^{265}Sg are expected, the significance of the observed event chains had to be improved. Therefore, a mother–daughter recoil mode for ROMA was implemented. In this mode, every second position on the wheel remains empty. Whenever an α -particle with the decay energy of ^{265}Sg or ^{266}Sg (between 8.5 and 8.9 MeV) was detected in a bottom detector, it was assumed that the daughter nucleus, ^{261}Rf or ^{262}Rf recoiled out of the KCl deposit on the polypropylene foil into the top detector (KCl was the aerosol in the recluster unit). Such an event initiated the daughter search mode by causing a single step. In this mode, the sources were removed from the detector pairs and empty positions were moved in between. The system waited for 2 min for the decay of the daughter nuclides, before the parent mode was resumed.

Two correlations observed in the daughter mode allowed the clear identification of ^{265}Sg . In addition, one very significant triple correlation was observed in the parent mode. Furthermore, a clear signature for the decay chain $^{266}\text{Sg} \rightarrow ^{262}\text{Rf}$ was registered.

In 1996, the experiment was continued and the isothermal temperature was varied in order to determine $\Delta H_a^{0(T)}$ for the Sg compound. First, the volatility of WO_2Cl_2 was carefully re-examined under conditions that were identical to those of the actual Sg experiment. Short-lived W-isotopes were produced in the 119 MeV ^{22}Ne on ^{152}Gd reaction at the GSI UNILAC accelerator. A He/C-jet (1.0 l/min) was used to rapidly transport the reaction products to the chromatography apparatus. As reactive agents, 144 ml/min Cl_2 saturated with SOCl_2 at room temperature (20 ml/min) and 2 ml/min O_2 were added.

The Sg experiment was performed with a mixed $^{248}\text{Cm}/^{152}\text{Gd}$ target ($690 \mu\text{g}/\text{cm}^2$ ^{248}Cm , $22 \mu\text{g}/\text{cm}^2$ ^{152}Gd) at a ^{22}Ne beam energy of 123 MeV. The same quartz column with the same quartz wool plug in the same chromatography oven as in the preceding W experiment was used. SF decays and α -decays were registered with ROMA. Every 10 s, the wheel was stepped to move the collected activity between 7 pairs of PIPS detectors. Again the mother–daughter recoil mode with a daughter search time of 200 s was implemented. Simultaneously, the yield of short-lived W was monitored with an HPGe detector, in order to ensure that the chemical separation was proceeding with high chemical yield.

The yield curve measured for $^{168}\text{WO}_2\text{Cl}_2$ ($t_{1/2} = 51$ s) was compared to the Monte Carlo model, and an adsorption enthalpy $\Delta_{\text{ads}}H^\circ(\text{WO}_2\text{Cl}_2) = -96$ kJ/mol was determined, in good agreement with the previous measurement.

At 350 °C isothermal temperature and with a beam dose of 2.31×10^{17} , two decay chains attributed to ^{265}Sg and one decay chain attributed to ^{266}Sg were observed, confirming the earlier results where Sg decays were observed at 300 and 400 °C isothermal temperature. At the lower isothermal temperature of 250 °C, a beam dose of 5.22×10^{17} was accumulated without observing any decays of $^{265,266}\text{Sg}$. Nevertheless, at 250 °C isothermal temperature, ^{168}W was still detected at about 75 % of its yield at 350 °C and was used to monitor system performance [69].

The decay data observed online, together with additional correlations that were discovered in a careful offline analysis of the list-mode data, allowed calculation of [142] half-lives and production cross-sections for ^{265}Sg and ^{266}Sg (121 ± 2 MeV, 68 % c.i.):

$$^{265}\text{Sg}:t_{1/2} = 7.4^{+3.3}_{-2.7} \text{ s and } \sigma \cong 240 \text{ pb}$$

$$^{265}\text{Sg}:t_{1/2} = 21^{+20}_{-12} \text{ s and } \sigma \cong 25 \text{ pb}$$

In the yield-vs.-temperature curve, all ^{265}Sg events measured at 300, 350, and 400 °C isothermal temperature were summed in one datum point with corresponding error limits corresponding to 100 % relative yield. Thus, it was assumed that in the temperature interval from 300 to 400 °C Sg oxochlorides are passing through the column with maximum yield. At 250 °C isothermal temperature, 0 events were observed and the upper limit at 68 % confidence level corresponds to 1.84 events. The yield curve for $^{265}\text{SgO}_2\text{Cl}_2$ from the Monte Carlo model that best fits the experimental data defines $\Delta_{\text{ads}}H^\circ(\text{SgO}_2\text{Cl}_2) = -100 \pm 4$ kJ/mol [69]. The uncertainty of 4 % given in [69] depends only on the event statistics and on the error limits of the half-life and is probably much too small as it does not include any systematic errors based on a number of assumptions inherent in the Monte Carlo model. However, as these are relevant in a similar way for the Mo, W, and Sg results, the resulting relative volatility sequence of the group 6 dioxodichlorides, $\text{MoO}_2\text{Cl}_2 > \text{WO}_2\text{Cl}_2 \geq \text{SgO}_2\text{Cl}_2$, is believed to be significant.

Thus, Gäggeler et al. [69] have determined the first relative thermodynamic property of an oxochloride of Sg, thereby ascertaining that the stoichiometry is SgO_2Cl_2 . The fact that the pseudogroup 6 element uranium forms another type of molecule, UCl_6 , under the experimental conditions, shows that the similarity of the first two transactinides, Rf and Db, to the early actinides thorium

and protactinium observed under certain chemical conditions [27], does not continue for uranium and the group 6 element Sg [43].

The other gas chromatography approach that has been developed [137] and recently been applied [148] to Sg is the online high-temperature gas chromatography of group 6 elements in the $O_2-H_2O(g)-SiO_2(s)$ system. S. Hübener, A. Vahle et al. have found that Mo and W are volatile in humid oxygen gas at relatively high temperatures and that the peculiar adsorption behavior both in the thermochromatography and in the isothermal gas chromatography [144–146], (for a detailed account see [147]), required the assumption of a dissociative adsorption and associative desorption



also called “reaction gas chromatography”. Relative elution yield of ^{169}W as a function of column temperature in isothermal online gas chromatography at $p(H_2O) = 780 \text{ Pa}$, $v_0(He) = 1 \text{ l min}^{-1}$, $v_0(O_2) = 0.5 \text{ l min}^{-1}$ [146] increases very slowly with increasing temperature and cannot be reproduced by the conventional model assuming reversible adsorption. The data can only be described by a Monte Carlo simulation for dissociative adsorption and associative desorption as formulated above with $\Delta_{diss,ads}H^\circ = -41 \text{ kJ/mol}$ and $\Delta_{diss,ads}S^\circ = -41 \text{ J/mol}\cdot\text{K}$. It is tempting to enlarge on this newly developed model.

The residence time of a molecule in the adsorbed state is a random quantity. Its expectation value is given by the Frenkel equation

$$\bar{\tau}_a = \tau_o \cdot e^{-\frac{\Delta_{ads}H^\circ}{RT}}$$

In the case of reversible adsorption, τ_o is the vibrational period of the adsorbed particle perpendicular to the surface of the adsorbing solid; it is typically of the order 10^{-12} – 10^{-14} s. In the case of reaction gas chromatography, $\bar{\tau}_a$ depends essentially on the kinetics of the velocity-determining associative desorption and the collision probability of water molecules with the adsorbed species.

The residence time in the adsorbed state becomes then

$$\bar{\tau}_a = \tau_o^* \cdot e^{-\frac{\Delta_{ads}H^\circ}{RT}}$$

If the volatility of the gaseous compound $[MO_2(OH)_2(g)]$ is much larger than that of the adsorbed species $[MO_3(ads)]$ the retention time t_r is equal to the total time of adsorption t_{ads} . This leads to the new expression for the retention time

$$t_r = \frac{L \cdot T_o \cdot F}{v_o T} \left\{ 1 + \frac{4}{d} \cdot \frac{c_{ads}^\circ(MO_3)}{c_{gas}(H_2O)} \cdot e^{-\frac{\Delta_{diss,ads}H^\circ}{RT}} \cdot e^{\frac{\Delta_{diss,ads}S^\circ}{R}} \right\}$$

with L = length of the isothermal part of the column

Φ = cross-section of the column

d = inner diameter of the column

$T_o = 298 \text{ K}$

T = isothermal temperature

$c_{ads}^\circ(MO_3)$ = standard concentration of MO_3 in the adsorbed state

$c_{gas}(H_2O)$ = concentration of water molecules

$\Delta_{diss,ads}H^\circ$ = standard enthalpy of the dissociative adsorption

$\Delta_{diss,ads}S^\circ$ = standard entropy of the dissociative adsorption

This equation tells two important things:

- i. an increase of the water partial pressure in the carrier gas leads to a higher collision probability of water molecules with the adsorbate, and
- ii. the new quantity τ_0^* becomes

$$\tau_0^* = \sqrt{\frac{2\pi M}{RT}} \cdot \frac{c_{\text{ads}}^\circ(\text{MO}_3)}{c_{\text{gas}}(\text{H}_2\text{O})} e^{\frac{\Delta_{\text{diss,ads}} S^\circ}{R}}$$

The latter equation means that, while τ_0 was only dependent on temperature and on properties of the adsorbing surface, τ_0^* depends on more parameters which are connected to the transport process [M molar mass of the transported species, $c_{\text{gas}}(\text{H}_2\text{O})$ and $\Delta_{\text{diss,ads}} S^\circ$]. Therefore, the values of τ_0^* can vary over large ranges and are always orders of magnitude larger than the values of τ_0 . For the transport of tungsten at a water partial pressure of 780 Pa, one obtains $\tau_0^* = 10^{-4}$ s.

The high temperatures that are necessary to obtain high yields (and fast transport [147]) have presented a technical challenge. Nevertheless, the system has been advanced such that a first application to the study of the volatility of Sg hydroxides was performed in 1998. This experiment [148], in which two decay chains of 21-s ^{266}Sg were observed, demonstrated that Sg, as with its higher homologs, forms a volatile $\text{SgO}_2(\text{OH})_2$ at elevated temperatures.

ARCA II [84], which has been successful in studying chemical properties of Db [27,81] and recently also of Rf [80,83] in aqueous solutions, was also selected to perform also the first aqueous chemistry with Sg [135].

Several chemical systems were tested with the fission products ^{93}Y , ^{97}Zr , and ^{99}Mo , and W isotopes produced in the $^{20}\text{Ne}+^{152}\text{Gd}$ reaction [135]. α -HIB solutions of 5×10^{-2} M, pH = 2.65 or pH = 5 used to elute W in a rapid, one-stage separation from cation-exchange columns provided a good separation from Hf and Lu [135]. Likewise [135], solutions with 0.1 M HCl and various HF concentrations between 10^{-4} and 10^{-2} M eluted W rapidly while Hf was safely retained on the column below 10^{-3} M HF. Hf was observed to be partially eluted for $\geq 2.8 \times 10^{-3}$ M HF in 0.1 M HCl. Finally, the decision was made to use 0.1 M $\text{HNO}_3/5 \times 10^{-4}$ M HF to elute a Sg fraction from cation-exchange columns [138] in order to avoid the formation of mixed chloride–fluoride complexes, which are difficult to model. $[\text{MO}_2\text{F}_3(\text{H}_2\text{O})]^-$ is a likely complex that is eluted, but neutral species such as MO_2F_2 cannot be excluded. Some problems were encountered with adsorption of the activities on the slider in ARCA II. Among the various materials tested, titanium showed the lowest losses of W and Hf due to adsorption.

The activity was transported to ARCA II with a He(KCl) jet within about 3 s and deposited on a titanium slider, dissolved and washed through the 1.6×8 mm chromatographic column (filled with the cation-exchange resin Aminex A6, 17.5 ± 2 μm) at a flow rate of 1 ml/min with 0.1 M $\text{HNO}_3/5 \times 10^{-4}$ M HF. 85 % of the W was eluted within 10 s. No di- or trivalent metal ions and no group 4 ions were eluted within the first 15 s. Also, uranium, in the form of UO_2^{2+} , was completely retained on the column.

In the Sg experiments [82a], a $950 \mu\text{g}/\text{cm}^2$ ^{248}Cm target was bombarded with 3×10^{12} ^{22}Ne ions s^{-1} at 121 MeV. 3900 identical separations were conducted with a collection and cycle time of 45 s and a total dose of 5.48×10^{17} ^{22}Ne ions. The transport efficiency of the He(KCl) jet was 45 %. On average, counting of the samples started 38 s after the end of collection. The overall chemical yield was 80 %. Three correlated $\alpha\alpha$ -mother–daughter decays were observed that are assigned to the decay of ^{261}Rf and ^{257}No as the decay products of ^{265}Sg . The three correlated events have to be compared with an expectation value of 0.27 for random correlations. This gives a probability of 0.24 % that the three events are random correlations. As the mother decays were not observed, it is important to note that ^{261}Rf and ^{257}No can only be observed if ^{265}Sg passed through the column because group 4 elements and No are strongly retained on the cation-exchange columns in ARCA II. Most likely, the decay of 7-s ^{265}Sg was not observed because it decayed in the time interval between the end of separation and

the start of measurement, which was equivalent to four half-lives. That the columns really retained ^{261}Rf was demonstrated recently in an experiment where ^{261}Rf was produced directly in the $^{248}\text{Cm}(^{18}\text{O},5\text{n})$ reaction [83], and processed in the Sg chemistry in 0.1 M $\text{HNO}_3/5 \times 10^{-4}$ M HF. ^{261}Rf did not elute from the column and was subsequently stripped from the column with 0.1 M $\text{HNO}_3/10^{-1}$ M HF.

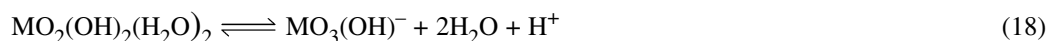
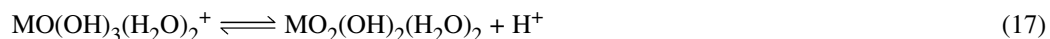
From the observation of the three correlated α -decay chains of ^{265}Sg daughters it was concluded that, for the first time, a chemical separation of Sg had been achieved in aqueous solution. Sg shows a behavior typical for a hexavalent element located in group 6 of the periodic table and different from that of the pseudo-group 6 element uranium, which is fixed as UO_2^{2+} on the cation-exchange column. Presumably, Sg forms $[\text{SgO}_2\text{F}_3(\text{H}_2\text{O})]^-$ or the neutral species $[\text{SgO}_2\text{F}_2]$, but due to the low fluoride concentration used, the anionic $[\text{SgO}_4]^{2-}$ ("seaborgate" in analogy to molybdate, $[\text{MoO}_4]^{2-}$, or tungstate, $[\text{WO}_4]^{2-}$) cannot be excluded.

In order to get experimental information on this latter question, a new series of Sg experiments with ARCA II was performed in 1996 in which 0.1 M HNO_3 without HF was used as the mobile aqueous phase and Aminex A6 as stationary phase [82 b]. If "seaborgate" was the ion isolated in 1995, it was expected to show up here again. A $690 \mu\text{g}/\text{cm}^2$ ^{248}Cm target containing $22 \mu\text{g}/\text{cm}^2$ enriched ^{152}Gd was bombarded with 123 MeV ^{22}Ne ions. The simultaneously produced ^{169}W served as a yield monitor. 45-s cycles were run, in which the effluent was evaporated on thin ($\sim 500 \mu\text{g}/\text{cm}^2$) Ti foils mounted on Al frames. These were thin enough to be counted in close geometry by pairs of PIPS detectors, thus increasing the efficiency for $\alpha\alpha$ -correlations by a factor of four as compared to the 1995 experiment. A beam dose of 4.32×10^{17} beam particles was collected in 4575 separations. Only one $\alpha\alpha$ -correlation attributable to the ^{261}Rf - ^{257}No pair was observed. With an expected number of random correlations of 0.5 this is likely (the probability is 30 %) to be a random correlation. From the beam integral and the overall yield as measured simultaneously for ^{169}W (27 % on average), a total of 5 correlated events was to be expected. This tends to indicate that, in the absence of fluoride ion, there is sorption of Sg in ARCA II.

This nontungsten-like behavior of Sg under the given conditions may be attributed [82b] to its weaker tendency to hydrolyze:



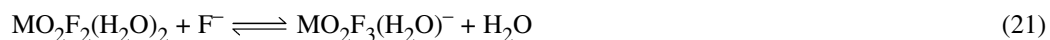
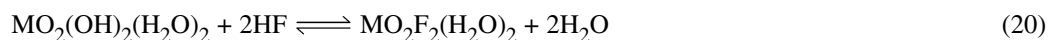
•
•
•



For Mo and W, the sequence of subsequent hydrolysis reactions in diluted HNO_3 reaches the neutral species $\text{MO}_2(\text{OH})_2(\text{H}_2\text{O})_2$. A weaker tendency to hydrolyze for Sg would stop this sequence earlier, e.g., with $\text{SgO}(\text{OH})_3(\text{H}_2\text{O})_2^+$, which sorbs on a cation-exchange resin.

It is interesting to recall that a decreasing tendency to hydrolyze ($\text{Nb} > \text{Ta} > 105 > \text{Pa}$) was reported [110] to determine the extraction of the group 5 chlorides into aliphatic amines. Thus, a similar behavior in the neighboring group 6 is conceivable, but needs to be verified.

In the presence of fluoride ions having a strong tendency to replace H_2O and OH^- ligands, the formation of neutral or anionic fluoride species is favored:



Thus, in the 1995 experiments [82a] with Sg in the presence of fluoride ions, neutral or anionic fluoride complexes (e.g., MO_2F_2 or MO_2F_3^-) were likely to be formed and were eluted from the cation-exchange columns. Experiments using the online three-column technique [87] are in preparation to determine the K_d value of Sg oxofluorides on an anion-exchange resin relative to the respective values for Mo and W [149].

Most recently, the chelating reagent α -HIB (0.05 M, unbuffered) was used to quickly elute Sg from cation-exchange columns in ARCA II [151]. In this system, Sg apparently behaves like Mo and W [135].

The centrifuge system SISAK-3 [89] was used to continuously extract a Sg fraction from an aqueous solution into an organic phase. In this phase, time-correlated α events were measured online by liquid scintillation counting (LSC) [90]. Homologs of Sg can be extracted from unbuffered 1 M α -HIB solution. The extractant was 0.046 M trioctylamine (TOA) dissolved in toluene, which contains dimethyl-POPOP and naphthalene as scintillator. The group 4 homologs of Rf remain in the aqueous phase [150].

The LSC spectroscopy provides an α -energy resolution of ~ 300 keV (FWHM) and nearly 100 % detection efficiency. Teflon cells (~ 7 ml volume) with meander-like structure were covered with an opaque quartz disk and were coupled to the photomultiplier with a cylindrical Teflon reflector. Pulse-shape discrimination (PSD) and pile-up rejection were applied to suppress background from β - and γ -radiation [90]. To increase the detection efficiency for α - α - α correlations in the ^{265}Sg - ^{261}Rf - ^{257}No decay chain, the detection system consisting of three consecutive counting cells was operated such that a trigger event in list mode in the 8.8 MeV region stopped the flow through that cell. The cell remained in the "daughter mode" for 2 min to wait for the decay of daughter nuclei. Owing to a relatively high β/γ background and a Po contamination, a number of random triple correlations resulted, yielding a detection limit of about 1 nb for the half-life region around 10 s. By digitizing and storing the shape of each event, it is hoped to improve the pile-up rejection by factors of 10–20 in forthcoming experiments.

7.3 Evaluation

Theoretical predictions concerning the chlorides and oxychlorides of the group 6 elements characterize MO_2Cl_2 as thermally more stable than MOCl_4 or MCl_6 [100,124–126] and suggest a volatility sequence $\text{MoO}_2\text{Cl}_2 > \text{WO}_2\text{Cl}_2 > \text{SgO}_2\text{Cl}_2$. Experimentally, the relative volatility sequence $\text{MoO}_2\text{Cl}_2 > \text{WO}_2\text{Cl}_2 \geq \text{SgO}_2\text{Cl}_2$ is found [69].

It was shown in addition [148] that Sg, as Mo and W, forms volatile oxide-hydroxides $\text{MO}_2(\text{OH})_2$ which are transported by "reaction gas chromatography". No values for the enthalpy and entropy of the dissociative adsorption on quartz surfaces are yet available.

In the aqueous phase, SgO_2F_2 and/or SgO_2F_3^- are likely to be the species that are rapidly eluted from cation-exchange columns in 0.1 M $\text{HNO}_3/5 \times 10^{-4}$ M HF [83]. In the absence of fluoride ions, Sg sorbs to the resin. This indicates a weaker tendency of Sg to hydrolyze as compared to its lighter homologs, a tendency that is also observed in groups 4 and 5 and that is in agreement with theoretical considerations [110]. The determination of the K_d value of SgO_2F_3^- on an anion-exchange resin is still to be done.

In addition to the fluoride ion, α -HIB seems to be another suitable ligand for forming anionic complexes with Sg [151].

8. CONCLUSION

Enormous progress in the evaluation of the chemical properties of the transactinide elements has been made over the past 15 years. Before about 1985, only very few (on the order of 10) publications existed on chemical studies of transactinides; by 1999, this number has increased by roughly one order of magnitude. While the early studies of chemical properties of Rf and Db revealed only qualitative features,

many of the more recent investigations have yielded quantitative information, i.e., heats of adsorption in the gas-phase chemical studies, and distribution coefficients in the aqueous-phase studies. Moreover, relativistic quantum chemical calculations of the molecules, combined with fundamental physicochemical considerations of their interaction with the chemical environment, have become available, which allow for detailed predictions of the chemical properties of the heaviest elements. It is by mutual comparison of theoretical and experimental results that an understanding of the sometimes surprising properties of the transactinides arises. At this time, the chemistry of Rf, Db, and Sg is known in some detail, even though there are a number of open questions to be answered. It is likely that the chemical studies of the transactinides will soon be extended to Bh, and to Hs, and eventually to even heavier elements.

ACKNOWLEDGMENT

The author is indebted to P. Sach for help in preparing the manuscript.

REFERENCES

1. G. T. Seaborg. *Radiochim. Acta* **70/71**, 69 (1995).
2. G. T. Seaborg. *Radiochim. Acta* **61**, 115 (1993).
3. J. J. Katz, G. T. Seaborg, L. R. Morss. *The Chemistry of the Actinide Elements*, 2nd ed., Chapman and Hall, London (1986).
4. G. T. Seaborg and W. D. Loveland. *The Elements Beyond Uranium*, Wiley, New York (1990).
5. G. T. Seaborg. *Chem. Eng. News* **23**, 2190 (1945).
6. B. Fricke and W. Greiner. *Phys. Lett.* **30B**, 317 (1969).
7. V. Pershina and B. Fricke. In *Heavy Elements and Related New Phenomena*, W. Greiner and R. K. Gupta (Eds.), pp. 194–262, World Scientific, Singapore (1999).
8. V. Pershina. *Chem. Rev.* **96**, 1977 (1996).
9. I. Zvara, Yu. T. Chuburkov, R. Caletka, T. S. Zvarova, M. R. Shalaevsky, B. V. Shilov. *At. Energ.* **21**, 8 (1966); *J. Nucl. Energ.* **21**, 60 (1966); *Sov. J. At. Energ.* **21**, 709 (1966).
10. I. Zvara, Yu. Ts. Chuburkov, T. S. Zvarova, R. Caletka. *Sov. Radiochem.* **11**, 153 (1969); I. Zvara, Yu. Ts. Chuburkov, R. Caletka, M. R. Shalaevsky. *Sov. Radiochem.* **11**, 161 (1969).
11. Yu. Ts. Chuburkov, I. Zvara, B. V. Shilov. *Sov. Radiochem.* **11**, 171 (1969).
12. I. Zvara, V. Z. Belov, L. P. Chelnokov, V. P. Domanov, M. Hussonnois, Yu. S. Korotkin, V. A. Shegolev, M. R. Shalaevsky. *Inorg. Nucl. Chem. Lett.* **7**, 1109 (1971).
13. R. J. Silva, J. Harris, M. Nurmia, K. Eskola, A. Ghiorso. *Inorg. Nucl. Chem. Lett.* **6**, 871 (1970).
14. E. K. Hulet, R. W. Lougheed, J. F. Wild, J. H. Landrum, J. M. Nitschke, A. Ghiorso. *J. Inorg. Nucl. Chem.* **42**, 79 (1980).
15. I. Zvara, B. Eichler, V. Z. Belov, T. S. Zvarova, Yu. S. Korotkin, M. R. Shalaevsky, V. A. Shegolev, M. Hussonnois. *Sov. Radiochem.* **16**, 709 (1974).
16. I. Zvara, V. Z. Belov, V. P. Domanov, M. R. Shalaevsky. *Sov. Radiochem.* **18**, 328 (1976).
17. I. Zvara. In *Int. Congress of Pure and Applied Chemistry*, Hamburg, Sept. 1973, p. 73, Butterworths, London (1974). See also I. Zvara, in *Transplutonium Elements*, W. Müller and R. Lindner (Eds.), p. 11, North-Holland, Amsterdam (1976).
18. I. Zvara. *Radiochim. Acta* **38**, 95 (1985).
19. I. Zvara. *Isotopenpraxis* **26**, 251 (1990).
20. A. Türler. *Radiochim. Acta* **72**, 7 (1996).
21. O. L. Keller, Jr. and G. T. Seaborg. *Ann. Rev. Nucl. Sci.* **27**, 139 (1977).
22. E. K. Hulet. In *Actinides in Perspective*, N. M. Edelstein (Ed.), p. 453, Pergamon Press, Oxford (1981).
23. O. L. Keller, Jr. *Radiochim. Acta* **37**, 169 (1984).

24. R. L. Silva. In *The Chemistry of the Actinide Elements*, 2nd ed., J. J. Katz, G. T. Seaborg, L. R. Morss (Eds.), Vol. 2, p. 1085, Chapman and Hall, London (1986).
25. D. C. Hoffman. In *The Robert A. Welch Foundation Conference on Chemical Research XXXIV Fifty Years with Transuranium Elements*, Houston, Texas, 22–23 October 1990, p. 255, and Lawrence Berkeley Laboratory Report LBL-29815 (1990).
26. D. C. Hoffman. *Radiochim. Acta* **61**, 123 (1993).
27. J. V. Kratz. *Proc. Int. Conf. on Actinides*, Santa Fe, New Mexico, 19–24 September 1993, Elsevier, Amsterdam (1994), and *J. Alloys Comp.* **213/214**, 20 (1994).
28. J. V. Kratz. *Chemie in Unserer Zeit*, 29. Jahrg. Nr. 4, 194 (1995).
29. D. C. Hoffman. *Chem. Eng. News* **72** (18), 24 (1994).
30. M. Schädel. *Radiochim. Acta* **70/71**, 207 (1995).
31. G. Münzenberg. *Radiochim. Acta* **70/71**, 193 (1995).
32. P. Armbruster. *Ann. Rev. Nucl. Part. Sci.* **35**, 135 (1985).
33. G. Münzenberg. *Rep. Prog. Phys.* **51**, 57 (1988).
34. G. Herrmann. *Angew. Chem., Int. Ed. Engl.* **27**, 1417 (1988).
35. W. Reisdorf and M. Schädel. *Z. Phys.* **A343**, 47 (1992).
36. Yu. Ts. Oganessian. *J. Alloys Comp.* **213/214**, 50 (1994).
37. G. Münzenberg. In *Frontier Topics in Nuclear Physics*, W. Scheid and A. Sandulescu (Eds.), Plenum, New York (1995).
38. G. Münzenberg and S. Hofmann. In *Heavy Elements and Related New Phenomena*, W. Greiner and R. K. Gupta (Eds.), pp. 9–42, World Scientific, Singapore (1999).
39. Yu. Ts. Oganessian. In *Heavy Elements and Related New Phenomena*, W. Greiner and R. K. Gupta (Eds.), pp. 43–47, World Scientific, Singapore (1999).
40. J. V. Kratz, M. K. Gober, H. P. Zimmermann, M. Schädel, W. Bröchle, E. Schimpf, K. E. Gregorich, A. Türler, N. J. Hannink, K. R. Czerwinski, B. Kadkhodayan, D. M. Lee, M. J. Nurmia, D. C. Hoffman, H. Gäggeler, D. Jost, J. Kovacs, U. W. Scherer, A. Weber. *Phys. Rev. C* **45**, 1064 (1992).
41. M. Schädel, W. Bröchle, E. Schimpf, H. P. Zimmermann, M. K. Gober, J. V. Kratz, N. Trautmann, H. Gäggeler, D. Jost, J. Kovacs, K. W. Scherer, A. Weber, K. E. Gregorich, A. Türler, K. R. Czerwinski, N. J. Hannink, B. Kadkhodayan, D. M. Lee, M. J. Nurmia, D. C. Hoffman. *Radiochim. Acta* **57**, 85 (1992).
42. Yu. A. Lazarev, Yu. V. Lobanov, Yu. Ts. Oganessian, V. K. Utyonkov, F. Sh. Abdullin, G. V. Buklanov, B. N. Gikal, S. Iliev, A. N. Mezentsev, A. N. Polyakov, I. M. Sedykh, I. V. Shirikovskiy, V. G. Subbotin, A. M. Sukov, Yu. S. Tsyganov, V. E. Zhuchko, R. W. Lougheed, K. J. Moody, J. F. Wild, J. H. McQuaid. *Phys. Rev. Lett.* **73**, 624 (1994).
43. M. Schädel, W. Bröchle, R. Dressler, B. Eichler, H. W. Gäggeler, R. Günther, K. E. Gregorich, D. C. Hoffman, S. Hübener, D. T. Jost, J. V. Kratz, W. Paulus, D. Schumann, S. Timokhin, N. Trautmann, A. Türler, G. Wirth, A. Yakushev. *Nature* **388**, 55 (1997).
44. S. Hofmann, V. Ninov, F. P. Hessberger, P. Armbruster, H. Folger, G. Münzenberg, H.-J. Schött, A. G. Popeko, A. V. Yeremin, S. Saro, R. Janik, M. Leino. *Z. Phys. A* **354**, 229 (1996).
45. R. Guillaumont, J. P. Adloff, A. Peneloux. *Radiochim. Acta* **46**, 169 (1989).
46. R. Guillaumont, J. P. Adloff, A. Peneloux, P. Delamoye. *Radiochim. Acta* **54**, 1 (1991).
47. R. J. Borg and G. J. Dienes. *J. Inorg. Nucl. Chem.* **43**, 1129 (1981).
48. N. Trautmann. *Radiochim. Acta* **70/71**, 237 (1995).
49. M. Schädel, W. Bröchle, B. Haefner. *Nucl. Instrum. Methods Phys. Res., Sect. A* **264**, 308 (1988).
50. K. E. Gregorich, R. A. Henderson, D. M. Lee, M. J. Nurmia, R. M. Chasteler, H. L. Hall, D. A. Bennett, C. M. Gannett, R. B. Chadwick, J. D. Leyba, D. C. Hoffman, G. Herrmann. *Radiochim. Acta* **43**, 223 (1988).

51. H. W. Gäggeler, D. T. Jost, U. Baltensperger, A. Weber, J. Kovacs, D. Vermeulen, A. Türlér. *Nucl. Instrum. Methods Phys. Res., Sect. A* **309**, 201 (1991).
52. R. Günther, H. U. Becker, S. Zauner, A. Nähler, J. V. Kratz, M. Schädel, W. Brüchle, E. Jäger, E. Schimpf, B. Schausten. Institut für Kernchemie, Univ. Mainz, Jahresbericht 1994, IKMz 95-1, 7 (1995).
53. I. Zvara, Yu. Ts. Chuburkov, V. Z. Belov, G. V. Buklanov, B. B. Zakhvataev, T. S. Zvarova, O. D. Maslov, R. Caletka, M. R. Shalaevsky. *Sov. Radiochem.* **12**, 530 (1970); *J. Inorg. Nucl. Chem.* **32**, 1885 (1970).
54. I. Zvara, V. Z. Belov, V. P. Domanov, Yu. S. Korotkin, L. P. Chelnokov, M. R. Shalaevsky, V. A. Shchegolev, M. Hussonnois. *Sov. Radiochem.* **14**, 115 (1971).
55. S. N. Timokhin, A. B. Yakushev, Xu Honggui, V. P. Perelygin, I. Zvara. Rep. at the NRC-3 Int. Conf., Vienna, Sept. 1992, *J. Radioanal. Nucl. Chem., Lett.* **212**, 31 (1996).
56. A. B. Yakushev, S. N. Timokhin, M. V. Vedeneev, Xu Honggui, I. Zvara. *J. Radioanal. Nucl. Chem., Articles* **205**, 63 (1996).
57. I. Zvara, A. B. Yakushev, S. N. Timokhin, Xu Honggui, V. P. Perelygin, Yu. T. Chuburkov. *Radiochim. Acta* **81**, 179 (1998).
58. H. W. Gäggeler. *J. Radioanal. Nucl. Chem., Articles* **183**, 261 (1994).
59. O. Knacke, O. Kubaschewski, K. Hesselmann (Eds.). *Thermochemical Properties of Inorganic Substances II*, Springer-Verlag, Berlin (1991).
60. A. I. Morozov and E. V. Karlova. *Russ. J. Inorg. Chem.* **16**, 12 (1971).
61. V. P. Domanov and Kim U Jin. *Radiokhimiya* **31**, 19 (1989).
62. B. Eichler. *Radiochim. Acta* **72**, 19 (1996).
63. D. T. Jost, G. Buklanov, R. Dressler, B. Eichler, H. W. Gäggeler, M. Gärtner, M. Grantz, S. Hübener, V. Lebedev, D. Piguet, S. N. Timokhin, A. Türlér, M. V. Vedeneev, A. B. Yakushev, I. Zvara. 4th Int. Conf. on Nuclear and Radiochemistry (NRC-4), Saint Malo, Sept. 1996, Extended Abstracts, IPN Orsay, Vol. **1**, A-P14 (1996).
64. B. Eichler, V. P. Domanov, I. Zvara. *Dubna Report* P12-9454 (1976).
65. A. Türlér, H. W. Gäggeler, K. E. Gregorich, H. Barth, W. Brüchle, K. R. Czerwinski, M. K. Gober, N. J. Hannink, R. A. Henderson, D. C. Hoffman, D. T. Jost, C. D. Kacher, B. Kadkhodayan, J. Kovacs, J. V. Kratz, S. A. Kreek, D. M. Lee, J. D. Leyba, M. J. Nurmia, M. Schädel, U. W. Scherer, E. Schimpf, D. Vermeulen, A. Weber, H. P. Zimmermann, I. Zvara. *J. Radioanal. Nucl. Chem.* **160**, 327 (1992).
66. H. W. Gäggeler, D. T. Jost, J. Kovacs, U. W. Scherer, A. Weber, D. Vermeulen, A. Türlér, K. E. Gregorich, R. A. Henderson, K. R. Czerwinski, B. Kadkhodayan, D. M. Lee, M. J. Nurmia, D. C. Hoffman, J. V. Kratz, M. K. Gober, H. P. Zimmermann, M. Schädel, W. Brüchle, E. Schimpf, I. Zvara. *Radiochim. Acta* **57**, 93 (1992).
67. A. Türlér, B. Eichler, D. T. Jost, D. Piguet, H. W. Gäggeler, K. E. Gregorich, B. Kadkhodayan, S. A. Kreek, D. M. Lee, M. Mohar, E. Sylwester, D. C. Hoffman, S. Hübener. *Radiochim. Acta* **73**, 55 (1996).
68. M. Gärtner, M. Boettger, B. Eichler, H. W. Gäggeler, M. Grantz, S. Hübener, D. T. Jost, D. Piguet, R. Dressler, A. Türlér, A. B. Yakushev. *Radiochim. Acta* **78**, 59 (1997).
69. H. W. Gäggeler. Proc. Int. Conf. on Actinides, Baden-Baden, 21–26 September 1997, *J. Alloys Comp.* **271-273**, 277 (1998).
70. B. Eichler and I. Zvara. *Radiochim. Acta* **38**, 103 (1985).
71. K. E. Gregorich, R. A. Henderson, D. M. Lee, M. J. Nurmia, R. M. Chasteler, H. L. Hall, D. A. Bennett, C. M. Gannett, R. B. Chadwick, J. D. Leyba, D. C. Hoffman, G. Herrmann. *Radiochim. Acta* **43**, 223 (1988).
72. K. R. Czerwinski, K. E. Gregorich, N. J. Hannink, C. D. Kacher, B. Kadkhodayan, S. A. Kreek, D. M. Lee, M. J. Nurmia, A. Türlér, G. T. Seaborg, D. C. Hoffman. *Radiochim. Acta* **64**, 23 (1994).

73. K. R. Czerwinski, C. D. Kacher, K. E. Gregorich, T. M. Hamilton, N. J. Hannink, B. Kadkhodayan, S. A. Kreek, D. M. Lee, M. J. Nurmia, A. Türler, G. T. Seaborg, D. C. Hoffman. *Radiochim. Acta* **64**, 29 (1994).
74. A. Bilewicz, S. Siekierski, C. D. Kacher, K. E. Gregorich, D. M. Lee, N. J. Stoyer, B. Kadkhodayan, S. A. Kreek, M. R. Lane, E. R. Sylwester, M. P. Neu, M. F. Mohar, D. C. Hoffman. *Radiochim. Acta* **75**, 121 (1996).
75. C. D. Kacher, K. E. Gregorich, D. M. Lee, Y. Watanabe, B. Kadkhodayan, B. Wierczinski, M. R. Lane, E. R. Sylwester, D. A. Keeney, M. Hendriks, N. J. Stoyer, J. Yang, M. Hsu, D. C. Hoffman, A. Bilewicz. *Radiochim. Acta* **75**, 127 (1996).
76. C. D. Kacher, K. E. Gregorich, D. M. Lee, Y. Watanabe, B. Kadkhodayan, B. Wierczinski, M. R. Lane, E. R. Sylwester, D. A. Keeney, M. Hendriks, D. C. Hoffman, A. Bilewicz. *Radiochim. Acta* **75**, 135 (1996).
77. J. V. Kratz, H. P. Zimmermann, U. W. Scherer, M. Schädel, W. Bröchle, K. E. Gregorich, C. M. Gannett, H. L. Hall, R. A. Henderson, D. M. Lee, J. D. Leyba, M. J. Nurmia, D. C. Hoffman, H. Gäggeler, D. Jost, U. Baltensperger, Ya Nai-Qi, A. Türler, Ch. Lienert. *Radiochim. Acta* **48**, 121 (1989).
78. M. K. Gober, J. V. Kratz, H. P. Zimmermann, M. Schädel, W. Bröchle, E. Schimpf, K. E. Gregorich, A. Türler, N. J. Hannink, K. R. Czerwinski, B. Kadkhodayan, D. M. Lee, M. J. Nurmia, D. C. Hoffman, H. Gäggeler, D. Jost, J. Kovacs, U. W. Scherer, A. Weber. *Radiochim. Acta* **57**, 77 (1992).
79. H. P. Zimmermann, M. K. Gober, J. V. Kratz, M. Schädel, W. Bröchle, E. Schimpf, K. E. Gregorich, A. Türler, K. R. Czerwinski, N. J. Hannink, B. Kadkhodayan, D. M. Lee, M. J. Nurmia, D. C. Hoffman, H. Gäggeler, D. Jost, J. Kovacs, U. W. Scherer, A. Weber. *Radiochim. Acta* **60**, 11 (1993).
80. R. Günther, W. Paulus, J. V. Kratz, A. Seibert, P. Thörle, S. Zauner, W. Bröchle, E. Jäger, V. Pershina, M. Schädel, B. Schausten, D. Schumann, B. Eichler, H. W. Gäggeler, D. T. Jost, A. Türler. *Radiochim. Acta* **80**, 121 (1998).
81. W. Paulus, J. V. Kratz, E. Strub, S. Zauner, W. Bröchle, V. Pershina, M. Schädel, B. Schausten, J. L. Adams, K. E. Gregorich, D. C. Hoffman, M. R. Lane, C. Laue, D. M. Lee, C. A. McGrath, D. K. Shaughnessy, D. A. Strellis, E. R. Sylwester. *Radiochim. Acta* **84**, 69 (1999).
82. (a) M. Schädel, W. Bröchle, B. Schausten, E. Schimpf, E. Jäger, G. Wirth, R. Günther, J. V. Kratz, W. Paulus, A. Seibert, P. Thörle, N. Trautmann, S. Zauner, D. Schumann, M. Andrassy, R. Misiak, K. E. Gregorich, D. C. Hoffman, D. M. Lee, E. R. Sylwester, Y. Nagame, Y. Oura. *Radiochim. Acta* **77**, 149 (1997); (b) M. Schädel, W. Bröchle, E. Jäger, B. Schausten, G. Wirth, W. Paulus, R. Günther, K. Eberhardt, J. V. Kratz, A. Seibert, E. Strub, P. Thörle, N. Trautmann, A. Waldek, S. Zauner, D. Schumann, U. Kirbach, B. Kubica, R. Misiak, Y. Nagame, K. E. Gregorich. *Radiochim. Acta* **83**, 156 (1998).
83. E. Strub, W. Bröchle, B. Eichler, H. W. Gäggeler, J. P. Glatz, A. Grund, M. Gärtner, E. Jäger, D. Jost, U. Kirbach, J. V. Kratz, A. Kronenberg, Y. Nagame, M. Schädel, B. Schausten, E. Schimpf, D. Schumann, P. Thörle, K. Tsukada, A. Türler, S. Zauner. Institut für Kernchemie, Univ. Mainz, Jahresbericht 1998, IKMz 99-2, 12 (1999).
84. M. Schädel, W. Bröchle, E. Jäger, E. Schimpf, J. V. Kratz, U. W. Scherer, H. P. Zimmermann. *Radiochim. Acta* **48**, 171 (1989).
85. H. Bruchertseifer, B. Eichler, J. Estevez, I. Zvara. *Radiochim. Acta* **47**, 41 (1989).
86. Z. Szegłowski, H. Bruchertseifer, V. P. Domanov, B. Gleisberg, L. J. Guseva, M. Hussonnois, G. S. Tikhomirova, I. Zvara, Yu. Ts. Oganessian. *Radiochim. Acta* **51**, 71 (1990).
87. G. Pfrepper, R. Pfrepper, A. B. Yakushev, S. N. Timokhin, I. Zvara. *Radiochim. Acta* **77**, 201 (1997).
88. G. Pfrepper, R. Pfrepper, D. Krauss, A. B. Yakushev, S. N. Timokhin, I. Zvara. *Radiochim. Acta* **80**, 7 (1998).

89. H. Persson, G. Skarnemark, M. Skålberg, J. Alstad, J. O. Liljenzin, G. Bauer, F. Haberberger, N. Kaffrell, J. Rogowski, N. Trautmann. *Radiochim. Acta* **48**, 177 (1989); J. Alstad, G. Skarnemark, F. Haberberger, G. Herrmann, A. Nähler, M. Pense-Maskow, N. Trautmann. *J. Radioanal. Nucl. Chem.* **189**, 133 (1995).
90. B. Wierczinski, K. Eberhardt, G. Herrmann, J. V. Kratz, M. Mendel, A. Nähler, F. Rocker, U. Tharun, N. Trautmann, K. Weiner, N. Wiehl, J. Alstad, G. Skarnemark. *Nucl. Instrum. Methods. Phys. Res., Sect. A* **370**, 532 (1996).
91. B. Fricke. In *Structure and Bonding*, J. D. Dunitz et al. (Eds.), Vol. 21, p. 90, Springer Verlag, Berlin (1975).
92. J. P. Desclaux. *At. Data Nucl. Data Tables* **12**, 311 (1973).
93. J. P. Desclaux and B. Fricke. *J. Phys.* **41**, 943 (1980).
94. L. Brewer. *High Temp. Sci.* **17**, 1 (1984).
95. V. A. Glebov, L. Kasztura, V. S. Nefedov, B. L. Zhuikov. *Radiochim. Acta* **46**, 117 (1989).
96. E. Johnson, B. Fricke, O. L. Keller, Jr., C. W. Nestor, T. C. Tucker. *J. Chem. Phys.* **93**, 8041 (1990).
97. E. Eliav, U. Kaldor, Y. Ishikawa. *Phys. Rev. Lett.* **74**, 1079 (1995).
98. B. L. Zhuikov, V. A. Glebov, V. S. Nefedov, I. Zvara. *J. Radioanal. Nucl. Chem.* **143**, 103 (1990).
99. M. V. Ryshkov, V. A. Gubanov, I. Zvara. *Radiochim. Acta* **57**, 11 (1992).
100. V. Pershina and B. Fricke. *J. Phys. Chem.* **98**, 6468 (1994).
101. G. M. Ter-Akopyan, R. N. Sagaidak, A. A. Pleve, S. P. Tret'yakova, G. N. Buklanov. *Dubna Report P7-85-634* (1985).
102. A. Ghiorso, M. Nurmia, J. Harris, K. Eskola, P. Eskola. *Phys. Rev. Lett.* **22**, 1317 (1969).
103. B. Kadkhodayan, A. Tüler, K. E. Gregorich, P. A. Baisden, K. R. Czerwinski, B. Eichler, H. W. Gäggeler, T. M. Hamilton, N. J. Hannink, D. T. Jost, C. D. Kacher, J. Kovacs, S. A. Kreek, M. R. Lane, M. F. Mohar, M. P. Neu, N. J. Stoyer, E. R. Sylwester, D. M. Lee, M. J. Nurmia, G. T. Seaborg, D. C. Hoffman. *Radiochim. Acta* **72**, 169 (1996).
104. A. Ghiorso, M. Nurmia, K. Eskola, P. Eskola. *Phys. Lett.* **32B**, 95 (1970).
105. A. Yakushev, G. Buklanov, B. Eichler, H. W. Gäggeler, M. Grantz, S. Hübener, D. T. Jost, V. Lebdev, D. Piguet, S. Timokhin, A. Türler, M. V. Vedeneev, I. Zvara. 4th Int. Conf. on Nuclear and Radiochemistry (NRC-4), Saint Malo, Sept. 1996, Extended Abstracts, IPN Orsay, Vol. **1**, A-P26 (1996).
106. B. L. Zhuikov, Yu. T. Chuburkov, S. N. Timokhin, Kim U Jin, I. Zvara. *Radiochim. Acta* **46**, 113 (1989).
107. D. T. Jost, H. W. Gäggeler, Ch. Vogel, M. Schädel, E. Jäger, B. Eichler, K. E. Gregorich, D. C. Hoffman. *Inorg. Chim. Acta* **146**, 225 (1988).
108. B. Eichler, S. Hübener, H. W. Gäggeler, D. T. Jost. *Inorg. Chim. Acta* **146**, 162 (1988).
109. K. R. Czerwinski. Ph.D. thesis, University of California, Lawrence Berkeley Laboratory Report LBL-32233 (1992).
110. V. Pershina. *Radiochim. Acta* **80**, 65 (1998) and *Radiochim. Acta* **80**, 75 (1998).
111. B. Fricke, E. Johnson, G. M. Rivera. *Radiochim. Acta* **62**, 17 (1993).
112. V. Pershina, W. D. Sepp, B. Fricke, A. Rosen. *J. Chem. Phys.* **96**, 8367 (1992).
113. V. Pershina, W. D. Sepp, B. Fricke, D. Kolb, M. Schädel, G. V. Ionova. *J. Chem. Phys.* **97**, 1116 (1992).
114. V. Pershina, W. D. Sepp, T. Bastug, B. Fricke, G. V. Ionova. *J. Chem. Phys.* **97**, 1123 (1992).
115. V. Pershina and B. Fricke. *J. Chem. Phys.* **99**, 9720 (1993).
116. G. V. Ionova, V. Pershina, E. Johnson, B. Fricke, M. Schädel. *J. Phys. Chem.* **96**, 11096 (1992).
117. U. W. Scherer, J. V. Kratz, M. Schädel, W. Brüchle, K. E. Gregorich, R. A. Henderson, D. M. Lee, M. J. Nurmia, D. C. Hoffman. *Inorg. Chim. Acta* **146**, 249 (1988).
118. V. Pershina, B. Fricke, J. V. Kratz, G. V. Ionova. *Radiochim. Acta* **64**, 37 (1994).

119. B. Eichler. *Annual Report 1993, Labor für Radio- und Umweltchemie*, p. 38, Paul Scherrer Institut (1994).
120. B. Kadkhodayan. Ph.D. thesis, University of California, Lawrence Berkeley Laboratory Report LBL-33961 (1993).
121. J. Korkisch. *Handbook of Ion Exchange Resins: Their Application to Inorganic Analytical Chemistry*, Vol. IV, p. 257, CRC Press, Boca Raton, FL (1989).
122. V. Pershina. Private communication (1997).
123. W. Paulus. Dissertation, Universität Mainz (1997), GSI Diss. 97-09 (1997).
124. V. Pershina and B. Fricke. *J. Phys. Chem.* **99**, 144 (1995).
125. V. Pershina and B. Fricke. *J. Phys. Chem.* **100**, 8748 (1996).
126. V. Pershina, T. Bastug, B. Fricke. *GSI Scientific Report 1995*, **GSI 96-1**, 15 (1996).
127. R. Dressler, A. Türler, D. T. Jost, D. Piguet, B. Eichler, H. W. Gäggeler. *Labor für Radio- und Umweltchemie der Universität Bern und des Paul Scherrer Instituts, Annual Report 1994*, p. 45 (1995).
128. V. Pershina and B. Fricke. *Radiochim. Acta* **65**, 13 (1994).
129. A. Ghiorso, J. M. Nitschke, J. R. Alonso, C. T. Alonso, M. Nurmia, G. T. Seaborg, E. K. Hulet, R. W. Lougheed. *Phys. Rev. Lett.* **33**, 1490 (1974).
130. V. A. Druin, B. Bochev, Yu. V. Lobanov, R. N. Sagaidak, Yu. P. Kharitonov, S. P. Tretyakova, G. G. Gulbekian, G. N. Buklanov, E. A. Yerin, V. N. Kosyakov, A. G. Rykov. *Sov. J. Nucl. Phys.* **29**, 591 (1979).
131. S. Hofmann, V. Ninov, F. P. Hessberger, P. Armbruster, H. Folger, G. Münzenberg, H. J. Schött, A. G. Popeko, A. V. Yeremin, A. N. Andreyev, S. Saro, R. Janik, M. Leino. *GSI-Nachrichten* **02-95**, 4 (1995).
132. S. Hofmann, V. Ninov, F. P. Hessberger, P. Armbruster, H. Folger, G. Münzenberg, H. J. Schött, A. G. Popeko, A. V. Yeremin, A. N. Andreyev, S. Saro, R. Janik, M. Leino. *Z. Phys. A* **350**, 277 (1995).
133. S. Cwiok, S. Hofmann, W. Nazarewicz. *Nucl. Phys. A* **573**, 356 (1994).
134. K. E. Gregorich, H. L. Hall, R. A. Henderson, J. D. Leyba, K. R. Czerwinski, S. A. Kreek, B. A. Kadkhodayan, M. J. Nurmia, D. M. Lee, D. C. Hoffman. *Phys. Rev. C* **45**, 1058 (1992).
135. W. Bröchle, B. Schausten, E. Jäger, E. Schimpf, M. Schädel, J. V. Kratz, N. Trautmann, H. P. Zimmermann, H. Bruchertseifer, W. Heller. *GSI Scientific Report 1991*, **GSI 92-1**, p. 315 (1992).
136. H. W. Gäggeler, D. T. Jost, J. Kovacs, M. Schädel, W. Bröchle, U. Becker, J. V. Kratz, B. Eichler, S. Hübener. *GSI Scientific Report 1991*, **GSI 92-1**, p. 321 (1992).
137. S. Hübener, B. Eichler, U. Becker, J. V. Kratz, H. W. Gäggeler, D. T. Jost, J. Kovacs, M. Schädel, W. Bröchle, E. Jäger. *GSI Scientific Report 1991*, **GSI 92-1**, p. 320 (1992).
138. R. Günther, W. Paulus, A. Posledni, J. V. Kratz, M. Schädel, W. Bröchle, E. Jäger, E. Schimpf, B. Schausten, D. Schumann, R. Binder. Institut für Kernchemie, Univ. Mainz, Jahresbericht 1994, IKMz 95-1, p. 2 (1995).
139. Z. Patyk and A. Sobiczewski. *Nucl. Phys. A* **533**, 132 (1991).
140. B. Eichler, A. Türler, D. T. Jost, H. W. Gäggeler. *Labor für Radio- und Umweltchemie der Universität Bern und des Paul Scherrer Instituts, Annual Report 1993*, p. 42 (1994).
141. B. Eichler and H. W. Gäggeler. *Labor für Radio- und Umweltchemie der Universität Bern und des Paul Scherrer Instituts, Annual Report 1993*, p. 40 (1994).
142. A. Türler, R. Dressler, B. Eichler, H. W. Gäggeler, D. T. Jost, M. Schädel, W. Bröchle, K. E. Gregorich, N. Trautmann, S. Taut. *Phys. Rev. C* **57**, 1648 (1998).
143. J. V. Kratz. In The Robert A. Welch Foundation Conference on Chemical Research XXXXI The Transactinide Elements, Houston, Texas, 27–28 October 1997.
144. A. Vahle, S. Hübener, B. Eichler. *Radiochim. Acta* **69**, 233 (1995).

145. S. Hübener, A. Vahle, M. Böttger, A. Türler, B. Eichler, D. T. Jost, D. Piguet, H. W. Gäggeler. *Labor für Radio- und Umweltchemie der Universität Bern und des Paul Scherrer Instituts, Annual Report 1994*, p. 46 (1995).
146. A. Vahle, S. Hübener, R. Dressler, B. Eichler, A. Türler. *Labor für Radio- und Umweltchemie der Universität Bern und des Paul Scherrer Instituts, Annual Report 1995*, p. 33 (1996).
147. A. Vahle. Doctoral dissertation, Technische Universität Dresden (1996).
148. S. Hübener, M. Grantz, H. Nitsche, S. Taut, A. Vahle, B. Eichler, H. W. Gäggeler, D. T. Jost, A. Türler. "Physikochemische Charakterisierung der Elemente der 6. Gruppe im O_2 - $H_2O(g)$ / $SiO_2(s)$ -System", Poster P 1.10 presented at the Symposium of the Nuclear Chemistry Division, German Chemical Society (GDCh), at Dresden, 7–9 Sept. (1998).
149. A. Kronenberg, J. V. Kratz, A. Nähler, W. Brüchle, E. Jäger, M. Schädel, G. Pfrepper, H. W. Gäggeler, A. Türler. "On-line Chromatographie mit kurzlebigen W-Isotopen mit der Multi-Column-Technique", Institut für Kernchemie, Univ. Mainz, Jahresbericht 1998, IKMz 99-2, 10 (1999).
150. B. Wierczinski, J. Alstad, K. Eberhardt, B. Eichler, H. Gäggeler, G. Herrmann, D. Jost, A. Nähler, M. Pense-Maskow, A. V. R. Reddy, G. Skarnemark, N. Trautmann, A. Türler. *Radiochim. Acta* **69**, 77 (1995).
151. W. Brüchle, R. Angert, B. Fricke, K. E. Gregorich, R. Günther, W. Hartmann, E. Jäger, U. Kirbach, J. V. Kratz, A. Kronenberg, B. Kubica, H. Kudo, Zongwei Li, M. Mendel, R. Misiak, G. Montavon, Y. Nagame, A. Nähler, I. Nishinaka, H. Nitsche, W. Paulus, V. Pershina, M. Schädel, B. Schausten, E. Schimpf, D. Schumann, A. Seibert, E. Strub, Z. Szeplowski, W. Thalheimer, P. Thörle, N. Trautmann, A. Waldek, G. Wirth, S. Zauner, A. v. Zweidorf. "Aqueous Chemistry with Seaborgium (Element 106)", Institut für Kernchemie, Univ. Mainz, Jahresbericht 1998, IKMz 99-2, p. 14 (1999).